Advances in Colloid and Interface Science, 28 (1987) 65–108
Elsevier Science Publishers B.V., Amsterdam – Printed in The Netherlands

PREPARATION OF MONODISPERSED COLLOIDAL PARTICLES

TADAO SUGIMOTO

Ashigara Research Laboratories, Fuji Photo Film Co., Ltd., 210 Nakanuma, Minamiashigara-City, Kanagawa 250-01, JAPAN

CONTENTS

I. ABSTRACT

The procedures and the backgrounds for the formation of monodispersed colloidal particles are reviewed, along with the personal view of the author's own, by classifying a wide variety of the systems. This article consists of the size distribution control for uniform colloidal systems with typical examples, including homogeneous and heterogeneous systems, and the crystal habit control of monodispersed particles.

II. INTRODUCTION

The problems of how to get monodispersed colloidal particles (i.e., particles uniform in size, shape and composition) and how to control their definite crystal habits are of obvious importance not only in the field of physical chemistry dealing with dynamic behavior and stability of particulate systems, but also in industries including catalysts, ceramics, pigments, pharmacy, photographic emulsions, etc.

The major significance of monodispersed particles may be attributed to the uniformity in physico-chemical properties of individual particles in a dispersion system, which allows us to directly correlate the properties as a whole system with those of each particle and facilitates the theoretical approach. The industrial importance seems to be due to the potential capability for the precise control of their own properties.

Complying with so many scientific and practical demands, great efforts have been devoted to the problems regarding the preparation of well defined colloidal particles over the last several decades. Specifically, it has been shown by Matijević and his coworkers (ref. 1-8) that numerous colloidal dispersions of different metal (hydrous) oxide particles which are uniform in size, shape and composition can be prepared by homogeneous precipitation in closed systems, whereas Berry et al. (ref. 9-11) and Moisar and Klein (ref. 12) opened the way of precisely controlled preparation of monodispersed silver halides by the controlled double jet technique in open systems in the early 1960's.

On this subject, several review articles are now available; for instance, by Overbeek (ref. 13) and the author (ref. 14) in addition to those by Matijević cited above (ref. 1-8). From these articles, readers will notice remarkable advance in the field, but also will find that a great many factors have a decisive influence on the preparation of monodispersed colloidal particles, depending on the individual cases. Indeed, many kinds of trials and scrupulous techniques are normally needed, so far, to reach a fairly uniform system.

In view of these situations, it seems to be highly desirable to resolve the general requirements for the preparation of uniform and well defined colloidal particles which could lead us to a systematic understanding of the various cases apparently unrelated to each other.

Thus, the present article is an attempt to give consistent interpretations to the formation of well defined colloidal particles, specifically uniform in size and shape by reference to the current examples.

III. SIZE DISTRIBUTION CONTROL

A. Requirements for monodisperse colloidal systems

There are several general conditions to obtain monodisperse colloidal systems as follows:

1. Separation between nucleation and growth. Fig. 1a is the well known LaMer diagram (ref. 15). The concentration of solute (monomers) is built up in Stage I, for instance, by slow decomposition of inert compounds generating the monomers, or formation of some sparingly soluble complexes as precursors of the precipitates, or other means. During this state, no precipitation takes place. When the solute concentration C reaches C^*_{min} the nucleation stage (Stage II) sets in. In this stage, C still keeps climbing for a while and then turns down as a result of consumption of solute by the pronounced nucleation. When C reaches C^*_{min} again, the nucleation comes to an end. Finally, the growth stage (Stage III) ensues until the concentration of solute is lowered close to the solubility level Cs.

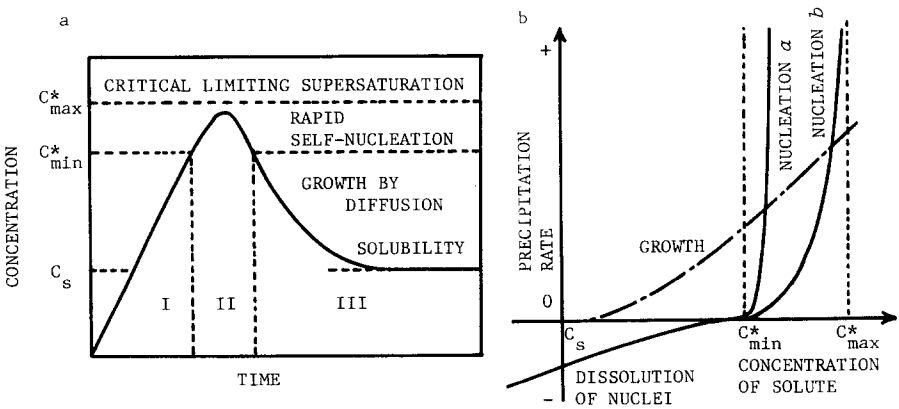

Fig. 1. (a) The LaMer model for monodispersed particle formation (C_s: solubility; C^*_{min}: minimum concentration for nucleation; C^*_{max}: maximum concentration for nucleation; I: prenucleation period; II: nucleation period; III: growth period) (ref. 15). (b) Precipitation rate for nucleation and growth as a function of solute concentration, where the growth curve is the one for a given amount of seed particles.

If the nucleation rate is not high enough (and thus the solute concentration C lingers between C^*_{min} and C^*_{max}), growth of the particles must occur at the same time. In such a case, a monodisperse dispersion may not be obtained. Thus, definite separation between the nucleation and the growth stages is the first requirement for uniform particle formation.

On the other hand, Fig. 1b is a diagram for precipitation rate versus solute concentration. If the nucleation rate soars as sharply as nucleation curve *a* imimediately after C exceeds C^*_{min} or if the slope of the growth curve is as low as the solute concentration at the intersection with the nucleation curve being close to C^*_{min}, the requirement will be ideally met. Needless to say, the most ideal situation is the combination of a strong dependence of the nucleation rate on supersaturation and a low growth rate. This is why the growth rates of monodispersed particles are mostly very low.

However, in a general case like nucleation curve *b*, the requirement would be satisfied only when C is limited to the level slightly above C^*_{min}, since C can soon get back below C^*_{min} following a short nucleation period. Thus, the long stay at a too-high supersaturation above C^*_{min} must be avoided for the homogeneous solution system to generate monodispersed particles.

One of the extreme measures to separate growth from nucleation may be the "seeding" as shown by Zsigmondy for gold colloids (ref. 16), where seed crystals are introduced into a monomer solution under a relatively low supersaturation below C^*_{min}.

In the author's opinion, the same effect may be realized by pH down for hydolyses of metal ions, dilution with solvent, addition of chelating agent, or a quick change of the tempeature immediately after a limited nucleation, which leads the higher supersaturation within the nucleation range to plunge into the lower supersaturation below C^*_{min} ("supersaturation quenching").

2. Inhibition of coagulation. Once particles are in direct contact, they often adhere to each other irreversibly; in some cases, they are subject to "contact recrystallization" (ref. 17). In the latter, particles in contact are cemented together by deposition of solute liberated from the other part of the particles onto the contact points. Thus, as a rule, inhibition of coagulation is necessary for the preparation of monodispersed particles.

a) Use of the electric double layer. As a typical measure against coagulation, it is well known that the electric double layers of charged particles exert repulsive force against each other which is a function of zeta potential and the Debye length. Accordingly, precipitation from a homogeneous solution is normally carried out in a range away from the point of zero charge and in a low ionic strength.

b) Use of gel network. If a gel-like precursor precipitates followed by nucleation of the final product thereon, all particles growing from the nuclei are expected to be pinned down on the substrate so that the interaction among them will be minimized. This effect appears to be involved in some heterogeneous systems (ref. 18,19) as will be discussed later in detail.

c) Use of protective agents. One of the most effective ways to stabilize lyophobic colloidal particles may be the use of protective agents, including

lyophilic polymers, surfactants and complexing agents, which are adsorbed on the particles; it is believed that stabilization occurs mainly through a repulsive force due to the Coulombic repulsion and/or the osmotic pressure and the steric hindrance at the overlapped regions of the adsorptive layers of the individual particles (ref. 20).

Thiele and Van Levern (ref. 21) evaluated the ability in stabilization of colloidal gold for many kinds of protective colloids, defining the "protective value". They found polyacrylic acid hydrazide, gelatin and poly-N-vinyl-5-methoxazolidon to be the most powerful protective agents.

3. Choice of growth modes. A colloidal particle grows by a sequence of monomer diffusion toward the surface and the reaction of monomers on the surface, as shown in Fig. 2a. Here, C_b is the bulk concentration of monomers, C_i is the monomer concentration at the interface, C_e is the solubility of the particle as a function of its radius and δ is the thickness of the diffusion layer as a function of the hydrodynamic shear due to the Brownian motion of the particle (ref. 22).

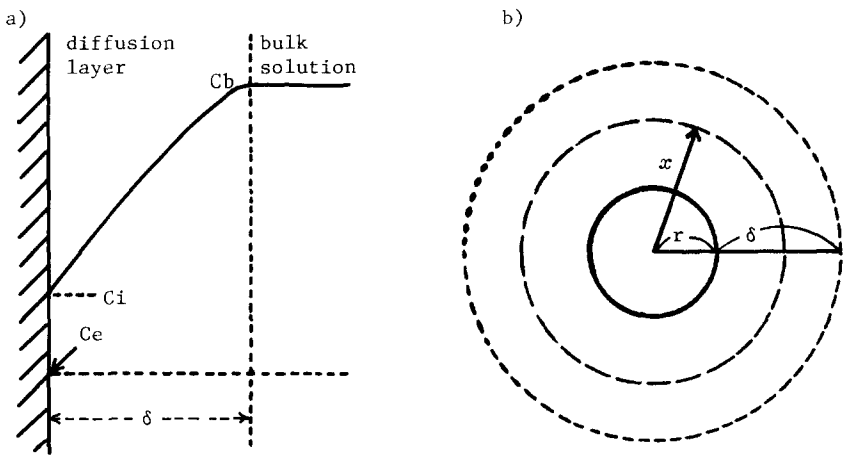

Fig. 2. (a) The profile of solute concentration in a diffusion layer. (b) The diffusion layer around a spherical particle.

Fig. 2b is the scheme of the diffusion layer around a spherical particle delineated from a more macroscopic viewpoint, where r is the particle radius and x is the distance from the center of the particle. The total flux of monomers, J, passing through a spherical surface with radius x within the diffusion layer is written by Fick's first law as:

$$J = 4\pi x^2 D \frac{dC}{dx} \quad , \tag{1}$$

where D is the diffusion coefficient and C is the monomer concentration at x. J is constant irrespective of x, inasmuch as the diffusion of monomers toward the particle is in a steady state. Thus, the integration of C(x) from $r + \delta$ to r with regard to x gives:

$$J = \frac{4\pi D r(r+\delta)}{\delta} (C_b - C_i) \quad . \tag{2}$$

Then the diffusion process is followed by the surface reaction written as:

$$J = 4\pi r^2 k(C_i - C_e) \quad , \tag{3}$$

where a simple first-order reaction is postulated and k is the rate constant. It follows from Eqs. 2 and 3 that:

$$\frac{C_i - C_e}{C_b - C_i} = \frac{D}{kr}\left(1 + \frac{r}{\delta}\right) \quad . \tag{4}$$

a) Diffusion-controlled growth. If $D \ll kr$ in Eq. 4, it follows that $C_i \simeq C_e$. In this case, the particle growth is controlled by the monomer diffusion ("diffusion-controlled growth"). Replacing C_i in Eq. 2 with C_e, one obtains that:

$$J = \frac{4\pi D r(r+\delta)}{\delta} (C_b - C_e) \quad . \tag{5}$$

J is related, on the other hand, with dr/dt as:

$$J = \frac{4\pi r^2}{V_m} \frac{dr}{dt} \quad , \tag{6}$$

where V_m is the molar volume of the solid; therefore, dr/dt can be written as:

$$\frac{dr}{dt} = DV_m\left(\frac{1}{r} + \frac{1}{\delta}\right)(C_b - C_e) \quad . \tag{7}$$

Eq. 7 means that dr/dt is lowered with an increase in r. In other words, the size distribution becomes narrower with particle growth if $(C_b - C_e)$ can be regarded virtually constant. In fact, the following relation is readily derived from Eq. 7:

$$\Delta r \propto 1 + \frac{\delta}{\tilde{r}} \quad , \tag{8}$$

where Δr is the standard deviation of the size distribution and $\tilde{r}$ is the mean particle radius. We are able to choose such a condition in some given systems as will be shown later.

b) Reaction-controlled growth. If $D >> kr$ in Eq. 4, then $C_b \cong C_i$ and the growth rate is limited by the surface reaction of monomers. Thus, one obtains from Eqs. 3 and 6 that:

$$\frac{dr}{dt} = kV_m(C_b - C_e) \quad . \tag{9}$$

Eq. 9 means that dr/dt is independent of the particle size and that Δr remains constant throughout the growth. As a consequence, the relative standard deviation, $\Delta r/\tilde{r}$, is reduced in the course of growth. This is the case when solute monomers simply deposit on a particle surface without any two-dimensional diffusion to form an amorphous solid or when the two-dimensional growth range of each nuclear step on a microcrystal is fairly limited by the fast nucleation on the surface. The latter case is the so called "polynuclear-layer growth" (ref. 23).

However, if the two-dimensional growth of the nuclei on the surface of a particle is extremely rapid as compared to the two-dimensional nucleation rate, the whole surface of the particle will be covered with a new solid layer initiated by a single nucleus. This reaction mode is referred to as "mononuclear-layer growth" (ref. 23). In this special case, dr/dt is proportional to the surface area of the particle as:

$$\frac{dr}{dt} = k'r^2 \quad . \tag{10}$$

Thus, the size distribution must get broader with the progress of particle growth. From Eq. 10, one may notice that this mechanism is possible (if at all) only in the very early stage of particle growth since otherwise r reaches infinity in a finite time (i.e., $r^{-1} = r_o^{-1} - k't$).

4. Gibbs-Thomson effect. Strictly speaking, the term $C_b - C_e$ in Eqs. 7 and 9 is not independent of the particle size, inasmuch as C_e is a function of the particle radius based on the Gibbs-Thomson equation:

$$C_e = C_\infty \exp\left(\frac{2\sigma V_m}{rRT}\right) \quad . \tag{11}$$

where C_∞ is the solubility of the solid with infinite dimensions, σ is the specific surface energy, R is the gas constant and T is the absolute temperature.

If $2\sigma V_m/rRT << 1$, C_e is approximated as:

$$C_e \cong C_\infty\left(1 + \frac{2\sigma V_m}{rRT}\right) \quad . \tag{12}$$

C_b is written likewise as:

$$C_b \cong C_\infty\left(1 + \frac{2\sigma V_m}{r^*RT}\right) \quad , \tag{13}$$

where r^* is the particle radius in equilibrium with the bulk solution.

In the case of a typical diffusion-controlled growth with the infinite diffusion layer ($\delta = \infty$ in Eq. 7), a combination of Eqs. 7, 12 and 13 yields:

$$\frac{dr}{dt} = \frac{K_D}{r}\left(\frac{1}{r^*} - \frac{1}{r}\right) , \tag{14}$$

where:

$$K_D = \frac{2\sigma D V_m^2 C_\infty}{RT} \tag{15}$$

Under a constant r^*, one obtains from Eq. 14 that:

$$\frac{d(\Delta r)}{dt} \cong \frac{K_D \Delta r}{\tilde{r}^2}\left(\frac{2}{\tilde{r}} - \frac{1}{r^*}\right) , \tag{16}$$

where a rather narrow size distribution is assumed, while Δr is the standard deviation of the size distribution and $\tilde{r}$ is the mean particle radius. Accordingly, it follows that

$$\begin{aligned} &\frac{d(\Delta r)}{dt} > 0 \qquad \text{for } \frac{\tilde{r}}{r^*} < 2 , \\ &\frac{d(\Delta r)}{dt} \leqq 0 \qquad \text{for } \frac{\tilde{r}}{r^*} \geqq 2 . \end{aligned} \tag{17}$$

Thus, if $\tilde{r}/r^*$ is less than 2, Δr tends to increase; i.e., the size distribution becomes broader under low supersaturation. This seems to be the underlying physical meaning of the Gibbs-Thomson effect reported by Wey and Strong (ref. 24), making the size distribution broader even in diffusion-controlled growth.

On the other hand, Δr tends to decrease for $\tilde{r}/r^* > 2$; i.e., the size distribution becomes narrower with the progress of growth when the supersaturation is kept high enough as compared to the solubility of the particles of the mean size. This is in accord with the aforementioned general trend of diffusion-controlled growth where the Gibbs-Thomson effect was ignored. These situations may be readily understood with the diagram of Fig. 3. Therefore, the bulk concentration of solute, C_b, should be set as high as just below the critical supersaturation in order to promote monodispersity in diffusion-controlled growth.

In the case of simple first-oder reaction-controlled growth, dr/dt may be written from Eqs. 9,12 and 13 as:

$$\frac{dr}{dt} = K_R\left(\frac{1}{r^*} - \frac{1}{r}\right) , \tag{18}$$

where:

$$K_R \equiv \frac{2\sigma k V_m^2 C_\infty}{RT} \qquad (19)$$

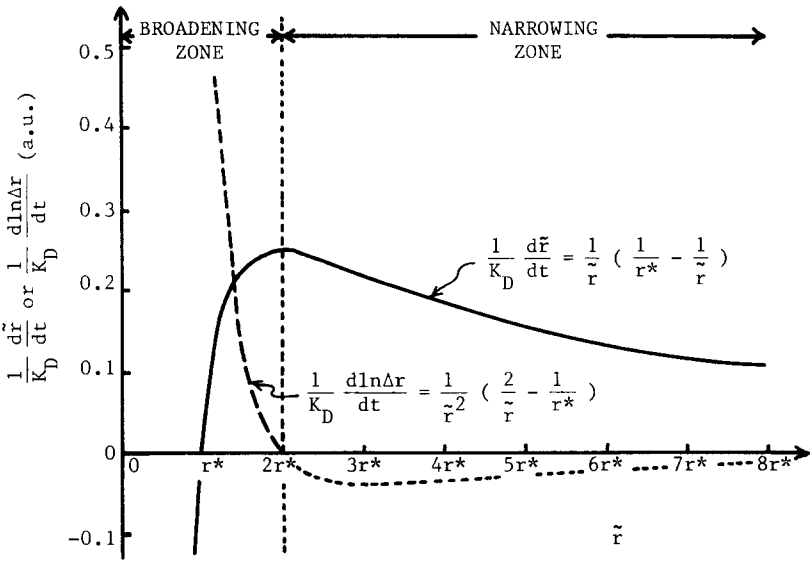

Fig. 3. $[d\tilde{r}/dt]/K_D$ or $[d\ln(\Delta r)/dt]/K_D$ as a function of r for diffusion-controlled growth with the infinite diffusion layer; the size distribution is broadened for $\tilde{r} < 2r^*$, while narrowed for $\tilde{r} > 2r^*$.

Similarly, $d(\Delta r)/dt$ is given as:

$$\frac{d(\Delta r)}{dt} = \frac{K_R \Delta r}{\tilde{r}^2} \,. \qquad (20).$$

Thus, $d(\Delta r)/dt$ is positive for any r so that some broadening of distribution takes place all the time in the simple reaction-controlled growth due to the Gibbs-Thomson effect. In addition, since $d\Delta r)/dt$ is independent of r^*, the broadening effect is inevitable, no matter how high the supersaturation is.

5. Reserve of monomers. In order to reconcile the two conflicting demands of a moderate supersaturation and an ample quantity of monomers for high yield of product, monomer reservoirs should be built in in individual systems. For instance, complexing agents such as citric acid, EDTA, triethanolamine, etc., shield a large amount of multivalent metallic cations. Thus, if one of these complexes is employed as a solute, the too high supersaturation and the excessive ionic strength with multivalent cations can be moderated at the same time. These effects prevent both concurrent nucleation and coagulation in the growth stage without lowering the product

yield through constant release of the metal ions. In the same manner, thioacetamide works as a reservoir of sulfur for the preparation of metal sulfides; monomer droplets release the monomers into the aqueous medium in an emulsion polymerization systems and water solvent serves as a reservoir of hydroxide ions for the hydrolysis of metal ions in an aqueous solution at low pH. If hydrolysis has to be carried out in the neutral pH range because of the high solubility product of the solid, some buffer system may be required to keep the hydroxide concentration at an adequate level. Thus, the buffer system is a reservoir of hydroxide. Furthermore, a solid precursor acts as a reservoir of the solute in a heterogeneous sytems, where it precipitates in advance, followed by the transformation or the recrystallization to yield the final product.

Hence, some reservoir of monomers is mostly indispensable for a monodisperse system. The concrete examples will be shown in the next part.

B. Typical monodisperse systems

In this article, monodisperse systems are classified into the homogeneous system or the heterogeneous one according to the number of phases in a system. Essentially, the homogeneous system consists of one phase, where the monomer reservoir is normally built in in the form of solute. Precipitation of the final product takes place directly (at least outwardly) from the homogeneous solution. A large number of reactions belong to this category, such as: 1) the redox reaction; 2) precipitation by poor solvents; 3) direct reaction of ions; 4) reaction of chelates; 5) decomposition of compounds; 6) hydrolysis in organic media; and 7) hydrolysis in aqueous media.

The heterogeneous system is composed of more than one phase (mostly two) prior to the precipitation of the final product. The monomers are reserved in one or each of them, whereas the precipitation of the final product takes place in one of these phases. Various characteristic systems are included in this category, such as: 1) phase transformation through aqueous media; 2) recrystallization through aqueous media; 3) emulsion polymerization; 4) reaction in microemulsions; and 5) reaction in aerosols.

Typical examples of these monodisperse systems are summarized in the following section along with some elucidations which were tried as to the backgrounds of the individual cases.

1. Homogeneous systems

a) Redox reaction. Zsigmondy (ref. 25) obtained monodispersed gold (Au) sols by reducing chloroauric acid with formaldehyde. He also found that monodispersed gold colloids were readily produced by using Faraday's gold sols (ca. 3 nm in mean size) as seed crystals with high reproducibility (ref. 16).

Takiyama (ref. 26) and Turkevich et al. (ref. 27) improved Zsigmondy's method by reducing chloroauric acid with sodium citrate and obtained spherical gold particles of 200 Å in mean diameter with high uniformity. The citrate appeared to work as a protective agent against coagulation by adsorption of the gold surfaces. In addition, the extensive experimentation for the proper conditions of temperature and concentration of the reactants seems to be basically an endeavor to avoid the concurrent nucleation during growth.

Watillon et al. (ref. 28,29) obtained highly monodispersed selenium (Se) particles (40 ~ 500 nm) by reducing selenious acid with hydrazine (ref. 28) or hydroxamine (ref. 29) in the presence of foreign nuclei of gold.

Sapieszko and Matijević (ref. 30) prepared spherical nickel (Ni) particles with a narrow size distribution by reducing a Ni-EDTA complex with hydrogen peroxide in highly basic media at 250°C. Similar nickel particles were also obtained with hydrazine in place of hydrogen peroxide. In these systems, decomposition of EDTA and reduction of N^{2+} ions took place at the same time.

Ottewill and Woodbridge (ref. 31) obtained monodispersed silver bromide (AgBr) by reducing BrO_3^- with nitrous acid at pH 3 in the presence of silver ions.

McFadyen and Matijević (ref. 32) prepared monodispersed cuprous oxide (Cu_2O; 0.3 ~ 1.6 μm) by reducing a cupric tartrate complex with glucose. A hydrolysis reaction simultaneously proceeds in this process.

Chiu and Meehan (ref. 33) precipitated uniform sulfur (S) particles by oxidizing hydrogen sulfide in aqueous solutions with air. The growth kinetics were found to be a diffusion control so that the size distribution is considered to have gotten narrower as the sulfur paticles grew.

Joekes (ref. 34) obtained monodispersed ferric hydroxide ($Fe(OH)_3$) particles from iron pentacarbonyl oxidized with hydrogen peroxide in ethanol solutions. In this reaction, ethanol worked as a stabilizer of the particles against coagulation.

Many kinds of complexing agents are frequently employed in the above reactions to moderate the supersaturation and to stabilize the generated particles.

b) Precipitation by poor solvents. LaMer and Dinegar (ref. 15) precipitated mondispersed sulfur (S) particles from ethanol solutions of sulfur which was slowly diluted up to the critical supersaturation with water. This system is not perfectly homogeneous, since uniform dilution is not achievable. In fact, the concentration of sulfur in the ethanol solution and the addition rate of water were found to have a crucial influence upon the uniformity of the particles.

As a rule, in such a quasi-homogeneous system, one of the following conditions should be satisfied: 1) the dissolution rate of the nuclei which have precipitated during the addition of the poor solvent is high enough to keep the system virtually homogeneous until the critical supersaturation as a whole system is reached; or 2) the growth rate is so low that solely nucleation occurs during the addition of the poor solvent by the local high supersaturation and no nucleation takes place in the subsequent growth state owing to the strong dependence of the nucleation rate on supersaturation. In addition, vigorous agitation is recommended, which insures the reproducibility by quickly dissipating the local supersaturation in the domain where the poor solvent is added.

c) Direct reaction of ions. If the nucleation rate is so low as to give a perfect homogeneous solution on mixing the reactants, or if either of the above requisites for quasi-homogeneous systems is fulfilled, the direct reaction of ions can be used for our purpose.

Ginell et al. (ref. 35) prepared monodispersed silver chloride (AgCl) particles by mixing ammonium chloride and silver nitrate in 95% ethanol. The particles were stabilized by the negative charges on their surfaces with the adsorption of chloride in an excess of chloride.

Herak et al. (ref. 36) precipitated monodispersed lead iodate ($Pb(IO_3)2$) particles of about 100 nm by the slow addition of a dilute potassium iodate solution to a dilute lead nitrate solution. They obtained monodispersed particles of lanthanum iodate ($La(IO_3)_3$) as well in the same way (ref. 37).

Wilhelmy and Matijević (ref. 6,38) obtained monodispersed spherical ferric phosphate ($FePO_4$) particles from a mixed solution of ferric perchlorate (8.0×10^{-4}M) and phosphoric acid (3.0×10^{-2}M) aged at 40°C for 24 hr.

Uniform spherical particles of aluminum phosphate ($Al(OH)_2H_2PO_4$; crystalline) were also prepared from acidic solutions containing $Al(NO_3)_3$ and Na_2HPO_4 aged at an elevated temperature (98°C) (ref. 39).

In the last two cases, some hydrolysis process is obviously involved according to the final composition (ref. 39) and/or the analysis of the intermediate complexes (ref. 38).

d) Reaction of chelates. Chiu prepared monodispersed microcrystals of lead sulfide (PbS; cubes; ~100 Å) (ref. 40), cupric sulfide (CuS; hexagonal bipyramids; ~200 Å) (ref. 41) and zinc sulfide (ZnS; multifaceted spheres; 0.1 ~ 0.4 μm) (ref. 42) by introducing hydrogen sulfide gas into solutions of EDTA complexes of the corresponding metal ions for several minutes at room temperature.

EDTA appears to prevent both nucleation and coagulation during the particle growth by shielding the metal ions. Meanwhile, the EDTA complexes may liberate metal ions by degrees with the progress of precipitation. The

use of such complexes or chelates seems to be one of the most promising techniques to produce uniform particles, since it is relatively easy to meet every requirement for monodisperse systems.

e) Decomposition of compounds. LaMer and Barnes (ref. 43) obtained monodispersed sulfur (S) particles by decomposition of sodium thiosulfate with acid. The particles were so highly uniform that they were used as a material to test the light scattering theory (ref. 44-47).

Takiyama (ref. 48) prepared monodispersed spindly particles of barium sulfate ($BaSO_4$) by decomposing a Ba-EDTA complex with hydrogen peroxide (Fig. 4a). In this reaction, the initial concentration of the complex was found to be the decisive factor in separating nucleation and growth.

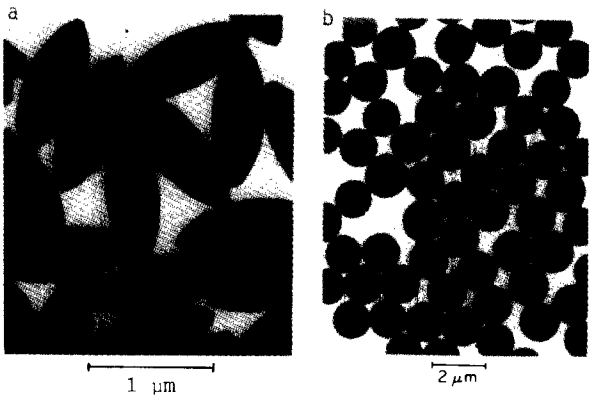

Fig. 4. (a) $BaSO_4$ particles precipiated by decomposition of Ba-EDTA complexes with H_2O_2 (ref. 48). (b) CdS particles obtained from a mixed solution of $Cd(NO_3)_2$ and thioacetamide, the latter of which is decomposed by HNO_3 (ref. 49).

Matijević and Wilhelmy (ref. 49) succeeded in the preparation of exceedingly monodispersed cadmium sufide (CdS) by decomposing thioacetamide with acid in the presence of cadmium ions. The particles were spherical and crystalline (Fig. 4b). They used seed crystals of cadmium sulfide to promote the monodispesity and found the kinetics to be a polynuclear layer reaction control from the analysis of Nielsen's chronomals (ref. 23). Thus, the relative standard deviation of the size distributoin must have been reduced during growth.

They also prepared uniform particles of zinc sulfide (ZnS; crystalline spheres) (ref. 50), lead sulfide (PbS; tetragonal galena) (ref. 51), cadmium zinc sulfide (CdS/ZnS; amorphous spheres and crystalline spheres) (ref. 51), and cadmium lead sulfide (CdS/PbS; crystalline polyhedra) (ref. 51) in a similar manner. The reason for the formation of crystalline spheres will be discussed later (see Part IV).

Gobet and Matijević (ref. 52) produced monodispersed particles of cadmium selenide (CdSe) and lead selenide (PbSe) by decomposition of selenourea in solutions of the corresponding metal salts. While both were crystalline, CdSe powders showed nearly spherical morphology whereas PbSe consisted of the particles of cubic symmetry.

Haruta and his coworkers (ref. 53) obtained spherical particles of molybdenum and cobalt sulfides with narrow size distribution by hydrolysis of thioacetamide promoted with hydrazine in solutions of ammonium orthomolybdate and cobalt (II) acetate, respectively. The particles which were obtained were of no distinct crystal structure as shown by X-ray diffraction analysis. These materials are of great importance as hydrodesulurization catalysts.

Janeković and Matijević (ref. 54) produced uniform rhombohedral cadmium carbonate ($CdCO_3$) particles by mixing a urea solution (~10M), preheated beforehand at 80°C for 24 hr. with an equal volume of dilute solution (2 x 10^{-3}M) of cadmium salt at room temperature. The carbonate ions which had been built up by preheating the urea solution brought about a single burst of nucleation on mixing with the solution of cadmium salt and gradual growth ensued. Thus, although the start of precipitation is rather inhomogeneous in this system, no further nucleation occurs after the initial one due to the low supersaturation of carbonate ions in the growth stage. Urea may play some roles for the formation of uniform rohmbohedral particles as a stabilizer and a habit modifier as well as a reservoir of carbonate ions.

They also prepared uniform and highly porous cadmium oxide (CdO) (ref. 54) particles by calcination of the uniform cadmium carbonate. After this heat treatment, the CdO particles still retained the original shape of the $CdCO_3$ but with high porosity.

Sapieszko and Matijević (ref. 55) produced disklike particles of hematite (α-Fe_2O_3) with a narrow distribution by decomposing a triethanolamine complex of ferric ions in solutions of high pH with hydrogen peroxide at 250°C.

Ottewill and Woodbridge (ref. 56) decomposed silver halide complexes in aqueous solutions by dilution with water and obtained monodispersed silver bromide (AgBr) and silver iodide (AgI) particles. These systems are not rigorously homogeneous since the homogeneous dilution was not realized in this method. Thus, they are basically the quasi-homogeneous systems so the mean size and the size distribution were strongly affected by the dilution and the agitation rates. The shape of the particles was different according to pAg (pAg = $-\log[Ag^+]$). At high pAg, the shape of AgBr was octahedral, whereas at low pAg, it was cubic. This will be discussed later in the section on crystal habit control (Part IV).

In those systems, the slow reactions of decomposition of chemical compounds were utilized to prepare uniform particles. Some organic compounds such as EDTA, triethanolamine, thioacetamide, selenourea, urea, etc., may protect the product particles against coagulation by adsorption to their surface and by shielding ionic species in addition to the role of monomer reservoirs which gradually release monomers to keep a moderate stationary concentration below the critical supersaturation in the growth stage.

f) Hydrolysis in organic media. Stöber et al. (ref. 57) prepared extremely uniform and spherical silica (SiO_2) particles by hydrolysis of tetraalkylsilicate and subsequent condensation of silicic acid in alcoholic solutions containing water and ammonia around room temperature. Ammmonia works as a catalyst of the hydrolysis and a modifier to make the particles spherical. The mean size ranges from 0.05 to 2 μm and any mean size can be chosen from this range by changing the compositions of water and/or ammonia and the kind of alcohols.

Uniform particles such as titanium dioxide (TiO_2) (ref. 58-60), barium titanium oxide ($BaTiO_3$) (ref. 61), zinc oxide (ZnO) (ref. 61) and zirconiuim dioxide (ZrO_2) (ref. 61-63) have also been generated by hydrolysis of the corresponding metal alkoxides in alcohol solutions. As-prepared metal oxide particles by this technique are normally amorphous and hydrated, whereas they are crystallized by calcination with the release of H_2O.

A method of this kind has several advantages; i.e.: 1) the simple and rapid reaction around room temperature; 2) the easy achievement of high purity of the product because it is free from inorganic anions of all kinds; and 3) the high yield of the product due to the allowance for the upper limit of the starting material concentration ($\sim 10^{-1}$M).

g) Hydrolysis in aqueous media. Demchak and Matijević (ref. 64) succeeded in the preparation of highly monodispersed spherical particles of chromium hydroxide ($Cr(OH)_3$) by hydrolysis of chromium ions in acidic aqueous media in 1969 (Fig. 5a). The novel genre of the preparation of uniform metal (hydrous) oxide particles has been extensively developed by Matijević and his coworkers since then (ref. 1-8).

Following the first preparation of the monodispersed chromium hydroxide sol, a number of uniform particles of metal (hydrous) oxide were produced in homogeneous systems; e.g., aluminum hydroxide [$Al(OH)_3$; amorphous spheres] (ref. 65-67), boehmite [α-AlOOH; crystalline clusters] (ref. 67), hematite [α-Fe_2O_3; crystalline ellipsoides, cubes, spheres and double spheres] (ref. 68-72), basic iron sulfate [$Fe_3(SO_4)_2 \cdot H_2O$; crystalline (hexagonal) truncated cubes and oblate spheroids] (ref. 73), titanium dioxide [TiO_2; crystalline (rutile) spheres] (ref. 74), basic thoriumsulfate [$Th(OH)_2SO_4 \cdot H_2O$;

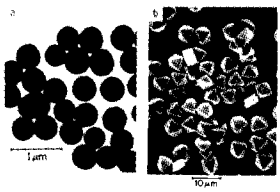

Fig. 5. (a) $Cr(OH)_3$ particles obtained by aging an acidic solution of chrome alum at 75°C for 24 hr. (ref. 64). (b) $Fe_3(SO_4)_2(OH)_5 \cdot 2H_2O$ particles obtained by aging an acidic solution of $Fe(NO_3)_3$ and $(NH_4)_2SO_4$ at 80°C for 1.5 hr. (ref. 73).

amorphous or polycrystalline spheres] (ref. 75), gallium hydrous oxide [amorphous spheres and crystalline rods] (ref. 76,77), manganese dioxide [δ-MnO_2] (ref. 78) and zirconium dioxide [ZrO_2; amorphous spheres] (ref. 79). The uniform and acicular particles of akageneite (β-FeOOH) prepared in the earlier studies by Watson et al. (ref. 80,81) appear to be classified into this category. As an application of the the method, uniform particles of maghemite [γ-Fe_2O_3; crystalline spindles] were also prepared by conversion from hematite of the same shape through a sequence of reduction-reoxidation processes (ref. 82). Most of them were prepared by heating dilute solutions ($10^{-4} \sim 10^{-2}$M) of metal salts over 50 to 150°C at low pH (1.0 ~ 4.0) for several hours or days.

The coagulation is prevented mainly by the repulsive force of the electric double layer exerted from the positively charged surfaces of each particle in the low pH range, which is effective at low ionic strength.

The surface reactions of these hydrolyses are generally slow so that they obey the reaction control kinetics; normally, the polynuclear-layer growth. Thus, the absolute standard deviation of size distribution is kept nearly constant throughout the growth stage, whereas the relative standard deviation against the mean particle radius is reduced by growth. Also, the low growth rate basically favors the separation between nucleation and growth. This separation is achieved by the proper choice of pH, temperature and anion species.

The low pH used in these systems is particularly important in order to keep a relatively low supersaturation with hydroxide ions which are constantly furnished by dissociation of water as their reservoir.

Also, high temperatures are normally employed for these systems. This is, of course, partly because it enhances the hydrolysis reaction, but what is more important is that some specific complexes of low solubility are often generated as precursors of the precipitates at elevated temperatures. Thus, it is not necessarily surprising that different products precipitate at times merely by the difference in temperature in otherwise identical systems (ref. 73,83).

Furthermore, the counterions to metal ions are known to play a definite role through the formation of their precursor complexes. For instance, monodispersed amorphous chromium hydroxide particles are generated from chromium salts of sulfate and phosphate, while no precipitation occurs if chloride, nitrate or perchlorate is used instead under the same condition (ref. 64,84,85). Sulfate and phosphate form many kinds of mixed complexes with chromium and hydroxide ions. As for sulfate, $[Cr_2(OH)_2SO_4)^{2+}$ and $Cr(OH)SO_4$ are believed to be the units of the precursor complexes (ref. 85). The nucleation of chromium hydroxide particles occurs as a result of the higher polymerization or the condensation of these precursor complexes with a release of sulfate ions. The bulky mixed complexes may not be suitable to form a crystal structure due to the steric hindrance and/or the lack of kinetic energy. This seems to be the reason why the uniform spherical particles of chromium hydroxide are amorphous.

Similarly, unless either sulfate or phosphate ions are used as counterions to aluminum ions, the product is not spherical aluminum hydroxide but is in the form of a rod, needle or unique cluster (ref. 65-67). Thus, anions are highly responsible for the morphology as well. As for the aluminum complexes, $Al_4(OH)_{10}SO_4$ is well known as their fundamental unit (ref. 86). The reaction mode is similar to that of chromium hydroxide so that the resultant particles are amorphous too (ref. 65-67) but an appreciable amount of sulfate is incorporated in the as-grown aluminum hydroxide particles in contrast with chromium hydroxide which is free of sulfate ions (ref. 65,85).

In the case of basic iron sulfate ($Fe_3(SO_4)_2(OH)_5$) (Fig. 5b), the complexes such as $Fe(OH)^{2+}$, $Fe_2(OH)_2^{4+}$ and $FeSO_4^+$ are claimed to be responsible for particle formation (ref. 83). Since these complexes initiate nucleation in the form of monomer or dimer, they appear to have a high degree of freedom and kinetic energy enough to form a crystal structure. In fact, they are known to be of hexagonal crystal symmetry. In this case, sulfate ions are built in as a component of the crystal lattice.

Anions other than sulfate and phosphate used for the hydrolysis of ferric ions at low pH normally give hematite (α-Fe_2O_3). However, the shape of the uniform hematite varies with anion species; e.g., nitrate and perchlorate give ellipsoids, whereas chloride yields cubes, spheres, ellipsoids, or double ellipsoids. However, rodlike β-FeOOH is also produced in a relatively higher concentration range of Fe^{3+} on aging of ferric chloride solutions (ref. 68). After all, the choice of counterions is of great importance for the hydrolysis of metal ions because some of them give no precipitate, while others decisively dominate the composition and the habitus of the final particles.

All procedures described above in this section are based on batch systems. However, a method is now also available for the continuous

preparation of uniform metal (hydrous) oxide particles by forced hydrolysis (ref. 87). Although the conditions for uniform particle formation in the continuous system are essentially the same as those in the batch technique, the former seems to be of more practical significance for industry.

Finally, it should be noted that there is some possibility of involvement of phase transformation or recrystallization in the formation of some metal oxides apparently precipitated from homogeneous solutions; e.g., it was found that rodlike β-FeOOH particles prevailed on short aging of ferric chloride in an acidic aqueous medium but on prolonged heating α-Fe_2O_3 was produced as the main product under certain conditions (ref. 68).

2. Heterogeneous systems

a) Phase transformation through aqueous media. In this system, a solid precursor different from the final product in composition precipitates beforehand from a heterogeneous solution and then it is dissolved to yield the more stable and uniform final particles.

Sugimoto and Matijević (ref. 18) prepared monodispersed cubic particles of cobalto-cobaltic oxide (Co_3O_4; 0.1 ~ 0.2 μm) with spinel structure by hydrolysis of cobalt (II) with partial oxidation of Co^{2+} ions over 90°C through 100°C for several hours, starting from an aqueous solution of ca. 10^{-2}M Co(II) acetate at pH 7.3. A green cobalt hydroxide gel precipitated at first and then the final particles formed thereon. The oxidation of Co^{2+} ions is caused by oxygen dissolved in the solution and thus it is extremely pronounced by bubbling oxygen or air. The counterions (acetate) work as a buffer of pH and also as a component of the precursor complexes for the Co_3O_4 (ref. 88). Too high pH (over 8) gave no precipitation of Co_3O_4 on the $Co(OH)_2$ gel so that a specific cobalt acetate complex free of OH^- (such as $CoAc^+$) may be responsible for the precipitation of the Co_3O_4 solid. The $Co(OH)_2$ gel serves as a gel network to hold each Co_3O_4 particle to prevent coagulation.

Sugimoto and Matijević (ref. 19) prepared monodispersed spherical magnetite (Fe_3O_4) as well by partial oxidation of ferrous hydroxide gel with nitrate. The uniform magnetite was obtained in slight excess of Fe^{2+} while the mean size critically depended on the Fe^{2+} concentration in excess, or pH.

First, the $Fe(OH)_2$ gel precipitated on mixing ferrous sulfate with potassium hydroxide. Then very fine magnetite particles (<0.1 μm) began to form on the gel by the introduction of potassium nitrate which is a mild oxidizing agent of ferrous ions. In the early stage, they increasd in number whereas no appreciable growth took place without coagulation among them, owing to the gel network. In the course of dissolution of the gel network with an accumulation of the primary particles, they suddenly started coagulation to form clusters as the nuclei of the secondary particles consisting of a limited number of primary particles. The secondary nuclei

promptly gathered the neighboring primary particles within the individual attraction fields, presumably by magnetic attraction in addition to van der Waals forces at pH close to the isoelectric point. The residual gel network might prevent coagulation among the isolated secondary particles to give monodispersed spherical magnetite particles. The formation process followed by electron microscopy and its schematic model are shown in Figs. 6 and 7, respectively.

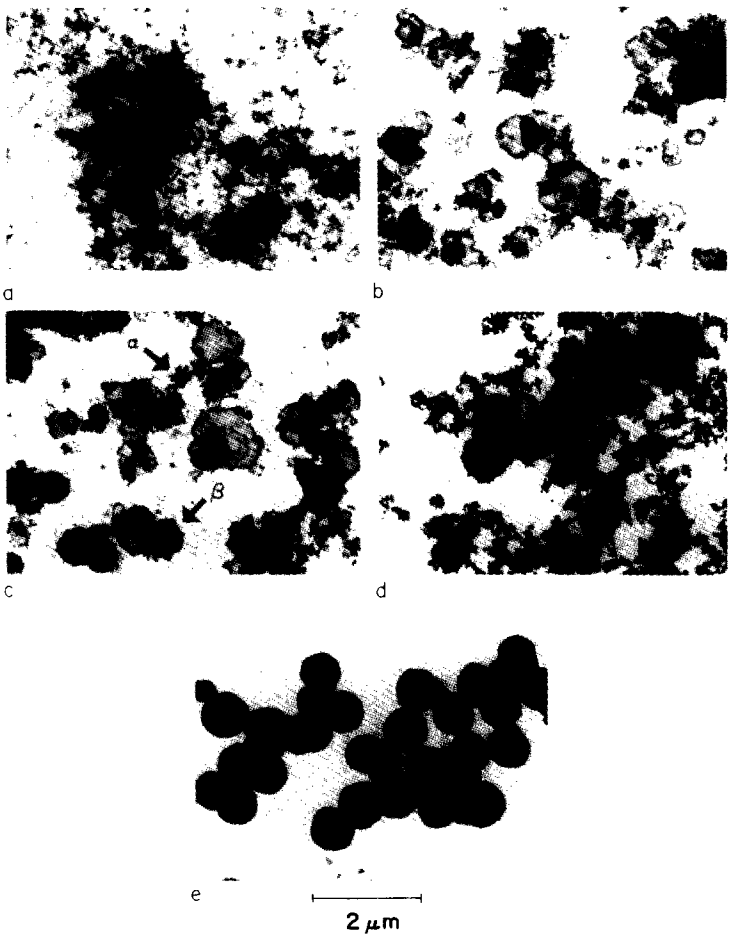

Fig. 6. Transmission electron micrographs for Fe_3O_4 formation in a system consisting of 2.5 x 10^{-2}M ferrous hydroxide and 5 x 10^{-3}M excess concentration of $FeSO_4$ aged at 90°C for: a) 0; b) 15; c) 30; d) 45; and e) 120 min. (ref. 19).

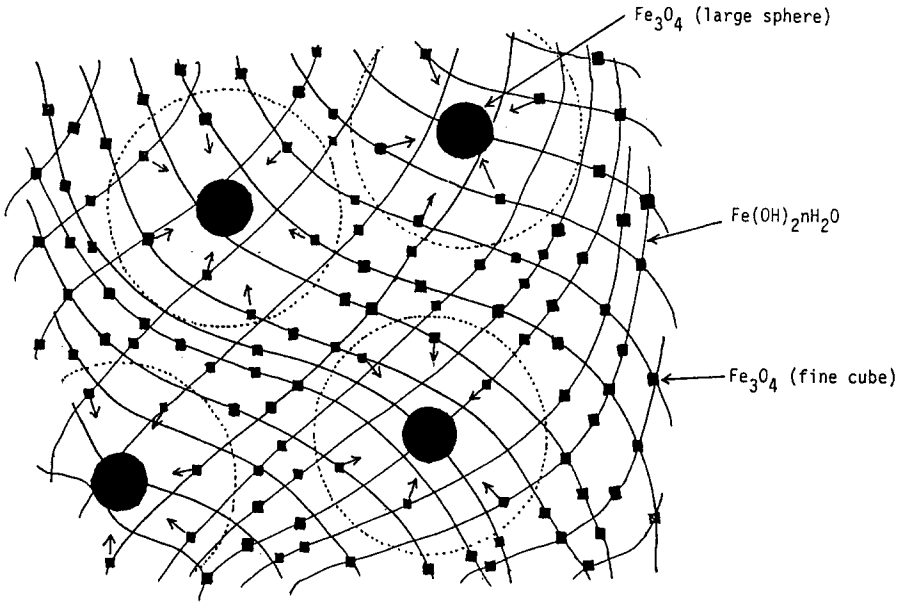

Fig. 7. The schematic model of the formation of Fe_3O_4 spherical particles.

The coagulation of the primary particles appears to be against the general rules for the formation of monodispersed particles. However, if the clustering of the primary particles is regarded as the nucleation of the secondary particles, this system is still in compliance with the rules.

It is not surprising that the particles obtained are spherical but crystalline, considering the formation process. In addition, the particles are supposed to be polycrystals composed of a substructure of the primary particles. The smooth surface of each particle was attributed to the rapid contact recrystallization of the constituent primary particles (ref. 17). The mean size of the particles is strongly dependent on the excess concentration of ferrous ions or pH, ranging from 0.03 to 1.1 μm. This may be due to the drastic change in the repulsive force of the electric double layer about the isoelectric point between the growing secondary particles and the neighboring primary ones. Similarly, monodispersed spherical ferrites of nickel (ref. 89), cobalt (ref. 90) and cobalt-nickel (ref. 91) were also obtained.

The gel-transformation method is applicable to other iron oxides. For instance, uniform spindle-type hematite (α-Fe_2O_3) was prepared from ferric hydroxide gel in the presence of phosphate and chloride ions (ref. 71). In this case, however, the positive role of the gel as a substrate of the final product is not definite since similar hematite particles were obtained as well in a homogeneous system in the presence of the same anions (ref. 71).

Hamada and Matijević (ref. 69) prepared uniform particles of cubic hematite (α-Fe_2O_3) by hydrolysis of ferric chloride in aqueous solutions of

alcohol (10-50%) at 100°C for several days. In this reaction, acicular crystals of β-FeOOH precipitate first and then they dissolve to form the cubic hematite. The intermediate, β-FeOOH, appears to work as a reservoir of the solute to maintain an ideal supersaturation for the nucleation and growth of the hematite. Since β-FeOOH as an intermediate and the cubic shape of the hematite are not peculiar to the alcohol/water medium (ref. 68), alcohol may favor the uniform particle formation as a poorer solvent in terms of the dielectric constant to give rise to a single burst of nucleation of hematite, apart from the subsequent growth process.

b) Recrystallization through aqueous media. Berry and his coworkers (ref. 9-11) obtained monodispersed silver bromide (AgBr) and silver chloride (AgCl) by simultaneous slow introduction of silver nitrate and the corresponding halide solutions into gelatin solutions. In this process, some constant precipitation of very fine primary nuclei of silver halide occurs in the domain of the gelatin solution where these reactant solutions are just injected. In the meantime, the primary nuclei are dispersed by agitation into the bulk solution region where relatively large stable nuclei grow at the expense of the smaller unstable nuclei by so called Oswald ripening (ref. 92,93). Thus, in this open system, a nucleation phase of the primary nuclei and a bulk phase for particle growth coexist in the same solution throughout the precipitation prcoess, as shown in Fig. 8. In the early stage, the number of stable nuclei increases with the growing supersaturation by the dissolution of the unstable nuclei and when a sufficient number of the slightly grown stable nuclei have been built up in the bulk phase, they become able to absorb the whole solute provided by the constant dissolution of all primary nuclei. From this moment, the growing particles cease to increase in number, whereas the primary nuclei generated in the nucleation phase begin to act simply as a monomer source. In other words, two distinct stages of the nucleation (i.e., accumulation of the stable nuclei) and growth are observed in the bulk phase which is analogous to the usual homogeneous systems. This is why the system can produce monodisperse particles. In this system, gelatin plays a definite role as a protective colloid to prevent coagulation among the primary nuclei as well as the growing particles at high ionic strength.

In addition, the silver bromide particles obey the diffusion-controlled growth mechanism within pBr 2.6 -3.5 ($pBr \equiv -\log[Br^-]$; $[Br^-]$ = excess concentration of bromide) (ref. 94), where we can take advantage of the specific reduction in size distribution.

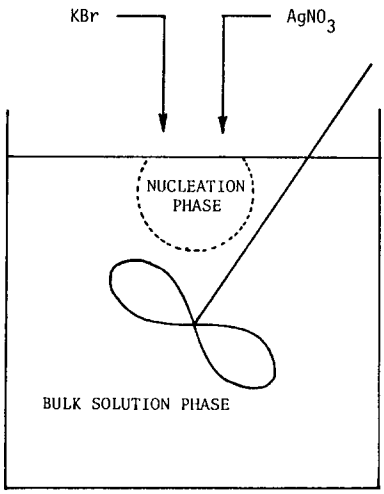

Fig. 8. Schematic model of the double-jet precipitation of photographic emulsions.

Furthermore, if the bulk concentration of solute is kept as high as just below the critical supersaturation throughout the precipitation by raising the addition rates of both silver nitrate and halide solutions with the particle growth, the broadening of the size distribution by the Gibbs-Thomson effect is expected to be minimized in the pBr range of diffusion control (see Part III-A-4). In fact, such an effect has been practically applied to the manufacture of silver halides (ref. 95,96).

c) Emulsion polymerization. Polystyrene latices produced by emulsion polymerization may belong to a group of most typically monodispersed colloids. They have been widely used as internal standards for electron microscopy (ref. 97,98), materials for the study of light scattering (ref. 99, 100), specimens for the study of interactions among colloidal particles (ref. 101,102), etc., because of their excellent uniformity.

According to Harkins (ref. 103) and Smith and Ewart (ref. 104) radical polymerization of monomers slightly dissolved in the water phase of a O/W emulsion is started by an initiator such as potassium persulfate and then the oligomer radicals are absorbed into the micelles of the emulsifier swollen with monomers due to the hydrophobic aliphatic hydrocarbon chains of the oligomers, followed by polymerization of the monomers in the micelles. This is the nucleation stage of emulsion polymerization. The polymer nuclei continue to grow with the monomers supplied from the monomer droplets stabilized by the emulsifier through the water phase of the emulsion. During this growth stage, the micelles of the emulsifier are decomposed to form an adsorbed surfactant layer on the polymer particles which stabilizes them. Decomposition of the micelles free from oligomer radicals may take place at

the same time and this appears to be a key to produce uniform particles owing to the absence of nucleation sites in the growth stage. In this mechanism, the monomer droplets work as a monomer reservoir (Fig. 9).

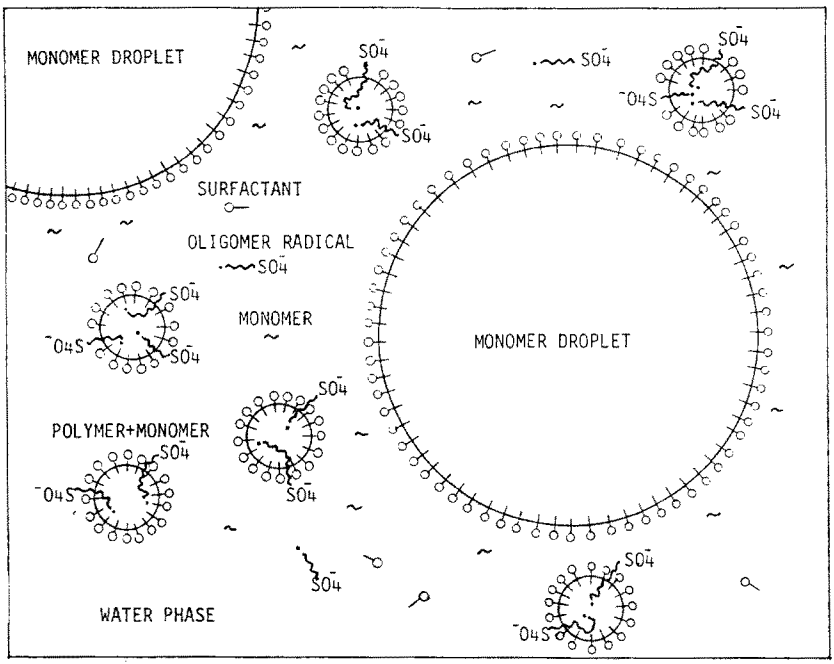

Fig. 9. Schematic model of emulsion polymerization.

Vanderhoff and his coworkers (ref. 105) found that the volume of the individual particles of a polystyrene latex grew at a rate proportional to the mean particle radius to the 2.0 - 2.5 power. This leads to narrowing of the relative width of size distribution during growth.

Some monodisperse latices, such as anionic polystyrene (ref. 106-108), cationic polystyrene (ref. 109), polymethylmethacrylate (ref. 110), styrene/acrylamide copolymers (ref. 111,112), etc., were also synthesized in the absence of emulsifiers. In these cases, the ionic oligomers may be further polymerized in the water phase to form solid nuclei by aggregation due to the hydrophobic long hydrocarbon chains, followed by their growth with the absorption of monomers through the aqueous medium. Even though some oligomerization may happen in the aqueous medium in the growth stage, the oligomers will be absorbed soon by the polymer particles. The ionic groups on the surfaces of individual polymer particles may stabilize them against coagulation of each other.

The "seeding" technique is recommended for emulsion polymerization as well to achieve high product uniformity. However, a too-high concentration

of emulsifier added to stabilize the seed particles results in rather polydisperse particles since it provides the system with free micelles as nucleation centers (ref. 105,113).

Recently, Ugelstad et al. have produced large (0.5 - 100 μm) monodispersed polymer spheres of polystyrene and its copolymers (ref. 114) and, in addition, nonspherical but uniform copolymer latices of polylstyrene/polyacrylate and polymethylmethacrylate/polyacrylate (ref. 115) by emulsion polymerization of the monodispersed polymer seeds swollen with the monomers.

Pendleton et al. (ref. 116) obtained monodispersed carbon particles (~-0.1 μm) by heat treatment or chemical dehydrochlorination of a uniform polyvinlyidene chloride latex prepared by emulsion polymerization (ref. 117). Specifically, the carbon particles obtained by heating at 700°C in a nitrogen atmosphere were highly porous and uniform but were subject to considerable shrinkage.

d) Reaction in microemulsions. Boutonnet et al. (ref. 118) obtained ultrafine monodispersed metal particles of the platinum group, including platinum (Pt), rhodium (Rh), palladium (Pd) and iridium (Ir) by reducing the corresponding salts in water pools of W/O microemulsions with hydrazine or hydrogen gas. Rapid reduction of the metal ions was a requisite to obtain the monodispersed particles. The mean particle size ranged from 3 to 5 nm with a narrow size distribution within 10% in relative standard deviation. They have a high potential for industrial application as catalysts.

Nagy et al. (ref. 119,120) prepared, as highly active catalysts for hydrogenation, uniform and very fine nickel boride and iron boride particles in W/O microemulsions of the CTAB/water/n-hexanol system by reducing the corresponding metal ions with sodium borohydride.

Kurihara et al. (ref. 121) obtained ultrafine uniform gold (Au) particles by radiolytic bombardment of $HAuCl_4$ in water pools of W/O microemulsions with a 353 nm laser pulse.

Gobe et al. (ref. 122) carried out hydrolysis of mixed solutions of ferrous and ferric ions with ammonia in W/O microemulsions to obtain ultrafine uniform particles of magnetite (Fe_3O_4). Similarly, monodispersed ultrafine particles such as silver chloride (AgCl) (ref. 123), barium carbonate ($BaCO_3$) (ref. 124). strontium carbonate ($SrCO_3$) (ref. 125), calcium carbonate ($CaCO_3$) (ref. 126) and silica (SiO_2) (ref. 127) have been produced by using a variety of chemical reactions in W/O microemulsions. Fig. 10 is an electron micrograph of ultrafine SiO_2 particles obtained by hydrolysis of tetraethoxyorthosilicate with ammonia in a W/O microemulsion of polyoxyethylene (6) nonylphenyl ether/water/cyclohexane system (ref. 127).

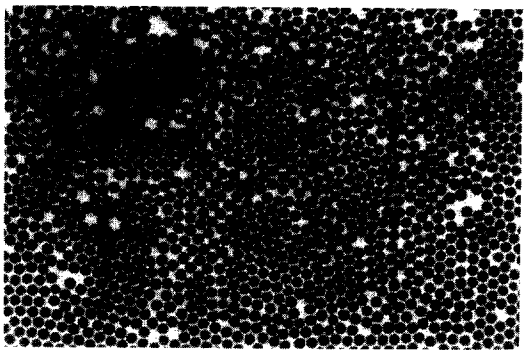

Fig. 10. Ultrafine SiO_2 particles obtained by hydrolysis of tetraethoxyorthosilicate in a W/O microemulsion of Np-6/water/cyclohexane system (ref. 127).

In this system, alkylsilicate and ammonia are separated in the oil and water phases, respectively, so that the direct mixing of the two reagents is avoided. In addition, the hydrolysis reaction is so slow as to give no appreciable precipitate on their mixing and to favor the separation between nucleation and growth. These are presumably why the highly uniform silica particles were produced.

In the meantime, ultrafine particles of polystyrene (200 - 400 Å) were prepared by polymerization in O/W microemulsions (ref. 128,129), whereas those of polyacrylamide (<500 Å) and its copolymers in W/O microemulsions (ref. 130-135).

Generally, the monodispersed particles prepared in microemulsions have the characteristics of very small mean size, narrow size distribution and high stability in the systems. However, the detailed mechanism for the formation of monodispersed fine particles in W/O microemulsions is yet to be resolved. For instance, the mass of each particle obtained by this method is normally much greater than the quantity of the monomeric species dissolved in individual water pools. This fact means that each water pool is not entirely isolated but repeats very rapid association and dissociation with each other. Thus, the monomeric species are freely exchanged among them; however, the resulting particles are monodispersed.

It seems to the author that extensive nucleation may occur in water pools in the early stage of precipitation since particle growth is strictly limited by strong adsorption of the surfactant which is tightly condensed about the water pools (~50 Å) in the form of reversed micelles. When a sufficient number of nuclei are built up so as to be able to absorb the monomeric species by their own growth, no further nucleation may take place and the

growth stage ensues by the exchange of monomeric species. As a result, the so obtained particles are very fine, whereas the separation between nucleation and growth is ideally realized to provide the particles with excellent uniformity. The coagulation among the particles must be prevented by the adsorption of surfactant. Thus, the water pools work as a monomer reservoir in addition to dispersed nucleation sites.

e) Reaction in aerosols. Matijević and his coworkers attempted hydrolysis of organic metal droplets with water vapor to produce monodispersed metal oxides in carrrier gases such as helium. They eventually succeeded in the preparation of monodispersed spherical particles (~0.2 μm) of titanium dioxide (TiO_2) (ref. 136), aluminum oxide (Al_2O_3) (ref. 137) and TiO_2/Al_2O_3 mixed particles (ref. 138) by hydrolysis of titanium and/or aluminum alkoxides. Titanium silicate (ref. 8) particles were also obtained by hydrolysis of mixed droplets of titanium ethoxide and silicon tetrachloride with water vapor. Fig. 11a is an electron micrograph of the TiO_2 particles obtained in an aerosol (ref. 136). The same technique was employed for the preparation of uniform particles of polystyrene and its derivatives (ref. 139) and divinylbenzene/ethylvinylbenzene copolymers (ref. 140) by polymerization of the corresponding monomer droplets in helilum carrier gas with a vaporized initiator (e.g., trifluoromethanesulfonic acid).

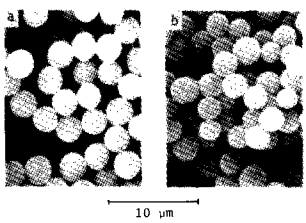

Fig. 11. (a) TiO_2 particles obtained by hydrolysis of titanium ethoxide droplets with water vapor (ref. 136). (b) Mixed polyurea-TiO_2 particles obtained by reaction of hexamethylene diisocyanate droplets with ethylenediamine vapor with subsequent exposure to titanium ethoxide vapor and hydrolysis with water vapor (ref. 141).

They also produced monodispersed polyurea and mixed polyurea-metal oxide particles (ref. 141). The polyurea particles were obtained by direct reaction of liquid droplets of diisocyanate with ethylenediamine vapor in the absence of any other additives. The particles obtained were further treated with metal alkoxide vapor, which on subsequent hydrolysis in a water vapor atmosphere resulted in mixed metal oxide/polyurea particles. For instance, titanium dioxide and aluminum oxide were incorporated in the organic cores by hydrolysis of the corresponding alkoxide vapors (Fig. 11b). Thus, these mixed particles are the products of the combination of gas phase polymerization and hydrolysis. They are readily dispersed in aqueous media.

The size distribution and the mean size of the solid particles are basically determined by those of the liquid droplets of the starting materials in aerosol systems. Thus, specific devices are concentrated on the generation of uniform liquid droplets, including the design of nebulizers, heterogeneous seeding of AgCl or NaCl (Sinclair-LaMer method [ref. 142-144]), temperature control, etc. (ref. 145-147). In other words, the formation of solid particles is simply a sort of conversion from the liquid droplets. The coagulation among liquid droplets is minimized by the spatial separation from each other and the quick solidification in the laminar flow of carrier gas.

IV. CRYSTAL HABIT CONTROL

It is not only of academic interest but of industrial importance as well to contemplate the mechanism of habit formation of uniform colloidal particles, inasmuch as the crystal habit is often responsible for the properties of colloidal particles; e.g., catalytic activity, photographic speed, magnetic properties, etc. Indeed, there are many intriguing problems left to be solved.

For instance, we have seen in the preceding sections not a few conflicting examples of spherical particles with definite crystal structures, such as CdS (ref. 49), ZnS (ref. 50), CdSe (ref. 52), $Al(OH)_2H_2PO_4$ (ref. 39), α-Fe_2O_3 (ref. 68), TiO_2 (ref. 74), Fe_3O_4 (ref. 19), etc. As for Fe_3O_4, the mechanism has been clearly elucidated from electron microscopy tracing the formation process; i.e., the prompt coagulation of fine primary particles, followed by contact recrystallization within the individual spherical particles (ref. 19). The polycrystalline substructure was also found for spherical hematite (α-Fe_2O_3) precipiated from homogeneous solutions of ferric chlorides (ref. 6). Spherical hematite is normally generated in a relatively high pH range with low ferric chloride concentration where β-FeOOH scarcely precipiates. This fact suggests that the highly hydrated and polymerized basic ferric chloride complexes and/or ferric hydroxide complexes may release water molecules following deposition onto the surfaces of the growing hematite particles to form very fine subcrystals just on the same spots without any extensive two-dimensional diffusion. This hypothesis could be extended to a general case in which some crystallization takes place within originally amorphous particles during their growth. In other words, the growing particles consist of a double structure of a crystalline core covered with an amorphous shell. The thickness of the shell may range from almost zero to the full radius, depending on the nature of the solid species and the environment. In any case, a number of nuclei for the crystallization must be dispersed within the amorphous shell of the particle while the subcrystals will grow on individual nuclei with random orientation until finally they complete a polycrystalline

spherical particle. The contact recrystallization may occur at the same time among the subcrystals to make the particle rigid and compact. The model is depicted in Fig. 12. This mechanism may explain the transition from amorphous to crystalline of the spherical mixed particles of ZnS/CdS simply by elevation of the temperature of preparation which enhances the crystallization process (ref. 51). The rough surfaces of the crystalline ZnS/CdS particles reveal their polycrystallinity. The same mechanism is also conceivable for the spherical particles of CdS (ref. 49) and ZnS (ref. 50) since such a rough surface is retained for CdS as well under certain conditions.

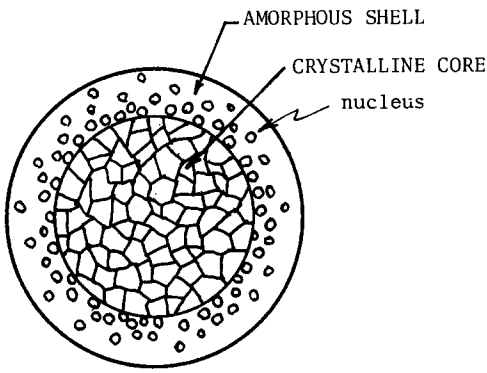

Fig. 12. Schematic model of spherical crystal formation.

On the other hand, the cubic hematite particle reported in ref. 68 and 69 is considered to be a single crystal from its characteristic habitus. It is normally produced by recrystallization from β-FeOOH precipiated beforehand in aqueous or alcohol/water solutions of ferric chloride of low pH (<2). The slow process under low supersaturation limited by the solubility of β-FeOOH appears to be in favor of the development of the single crystal since the surface reaction of crystallization can readily follow the deposition of the precursor complexes. The crystallization process must be promoted at high temperature (~150°C). In addition, since ferric chloride solute complexes of low molcular weight such as $FeCl(H_2O)_5^{2+}$ and $FeCl_2(H_2O)_4^{+}$ seem to be dominant under these conditions (ref. 166-168), they must also favor the formation of the single lattice structure with their high kinetic energy for surface diffusion and rearrangement, analogous to the formation of the basic iron sulfate (ref. 83). Alcohol is known to enhance the ferric chloride solute complexation (ref. 168).

Furthermore, it is well known that specific adsorption of ions, complexes, organic compounds, etc., brings about a variety of morphology of colloidal microcrystals by restraining or sometimes promoting growth of the facets to

which they are adsorbed (ref. 148-151); for instance: 1) disklike hematite produced in the presence of triethanolamine (ref. 55); 2) hexagonal particles of basic iron sulfate ($Fe_3(SO_4)_2(OH)_5 \cdot 2H_2O$) with corners and edges rounded off by excess sulfate ions (ref. 73); 3) octahedral silver bromide obtained by adsorption of bromide (ref. 12) or $AgBr_n^{(n-1)-}$ complexes (ref. 152); 4) morphological change of AgBr from octahedron to cube by adsorption of ammonia (ref. 153); 5) extraordinary shape of AgBr in rhombododecahedron, icositetrahedra, trisoctahedra, tetrahexahedra, or hexoctahedra formed by adsorption of organic compounds (ref. 154-156); and 6) the silver chloride particles in octahedron or rhombododecahedron in the presence of organic compounds such as dimethylthiourea or 2-(carboxymethylmercapto)-benzimidazole (ref. 57) or cations such as cadmium ions (ref. 158). However, little is known about the mechanism of habit modification of microcrystals despite its fundamental and practical importance. Thus, the rest of this section is to be devoted to an attempt at further insights into the problems of habit formation of uniform microcyrstals bound by their own typical facets.

Gibbs (ref. 159) suggested that a polyhedral crystal in equilibrium with the surroundings would assume a shape with the minimum surface free energy. This idea was formulated by Wulff (ref. 160) as follows:

$$\frac{\sigma_1}{r_1} = \frac{\sigma_2}{r_2} = \cdots = \frac{\sigma_i}{r_i} = \cdots = \frac{kT}{2\nu_m} \ln \frac{P}{P_o} \quad , \tag{21}$$

where σ_i and r_i are the specific surface energy of the ith face of the polyhedral crystal and the central distance to the face, respectively, k is the Boltzmann constant, ν_m is the molecular volume, P_o is the vapor pressure of a crystal of infinite dimensions, and P is the vapor pressure of the polyhedral crystal. The vapor pressures are replaced by the solubilities or equilibrium activities for a crystal in a solution. This is the concept of the "equilibrium form".

Meanwhile, Curie (ref. 161) considered that a crystal might grow under supersaturation, maintaining the equilibrium form with its minimum surface energy. However, his hypothesis has never been verified for the growth of real polyhedral crystals of large dimensions. This is partly because there is virtually no difference in vapor pressure or solubility between a large crystal and the infinite-sized one (i.e. $P \cong P_o$) so that Eq. 21 loses its significance, and partly because the shape of a crystal is determined by the difference in growth rate of the individual facets for the reaction-controlled growth (the growth form").

Consequently, it has been generally accepted that the equilibrium form is the ultimate crystal shape in equilibrium with the surroundings as a result of the recrystallization within the individual microcrystals in a closed system, whereas the growth form is a kinetic shape formed by the difference in growth rate constant among each facet of a crystal under a certain supersaturation. Thus, it seems to the author that the correlation between the two kinds of crystal forms has scarcely been discussed and that they have been treated as concepts independent of each other. Therefore, the author (ref. 162) has defined a thermodynamic quantity, "surface chemical potential", which enables us to deal with non-equilibrium forms as well as equilibrium forms and thus the problems on the correlation between them.

A. Surface chemical potential

Let us consider a simple tetradecahedral microcrystal bound by six {100} faces and eight {111} faces as illustrated in Fig. 13. The extreme shapes are the octahedron bound by {111} faces only and the cube bound by {100} faces only. Here tetradecahedron A is an intermediate form between the octahedron and tetradecahedron M while tetradecahedron B corresponds to a shape between tetradecahedron M and the cube.

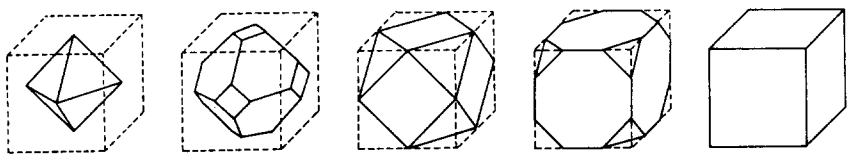

Fig. 13. An octahedron, tetradecahedron A, M and B and a cube (ref. 162).

The surface chemical potential (SCP) of a {100} face of a tetradecahedral microcrystal, μ_{100} , is now defined as a change of surface free energy of the microcrystal by the growth of the {100} face with one mole of the component molecules in the direction normal to the {100} face where the central distance to the {111} faces is fixed. The SCP of a {111} face is defined as well in an analogous manner. Meanwhile, the surface free energy of a tetradecahedron, G, is written as:

$$G = S_{100}\sigma_{100} + S_{111}\sigma_{111} \quad , \tag{22}$$

where S_{100} and S_{111} are the total surface area of the {100} and the {111} faces of the particle, respectively, and σ_{100} and σ_{111} are the specific surface energies of the respective faces. Thus, μ_{100} and μ_{111} are given as:

$$\left.\begin{aligned} \mu_{100} &= \left(\frac{\partial G}{\partial n}\right)_{r_{111}} = V_m\left(\frac{\partial G}{\partial r_{100}}\right)/\left(\frac{\partial \nu}{\partial r_{100}}\right) \quad , \\ \mu_{111} &= \left(\frac{\partial G}{\partial n}\right)_{r_{100}} = V_m\left(\frac{\partial G}{\partial r_{111}}\right)/\frac{\partial \nu}{\partial r_{111}} \quad , \end{aligned}\right\} \tag{23}$$

where n is the mole number of the constituent molecules of the particle, r_{100} and r_{111} are the central distances to the {100} and {111} faces, respectively, V_m is the molar volume of the solid and ν is the volume of the particle. S_{100}, S_{111} and ν are given as functions of r_{100} and r_{111} so that μ_{100} and μ_{111} are obtained as functions of the central distances and the specific surface energies. The SCP's for the {100} and the {111} faces are summarized in Table 1.

TABLE 1

Surface chemical potentials of {100} and {111} faces for tetradecahedra (ref. 162).

Types of tetradecahedra	μ_{100}	μ_{111}
Type A ($1/\sqrt{3} \le r_{111}/r_{100} \le 2/\sqrt{3}$)	$\frac{-2\sigma_{100} + 2\sqrt{3}\sigma_{111}}{\sqrt{3}r_{111} - r_{100}} V_m$	$\frac{2(\sqrt{3}r_{111} - r_{100})\sigma_{100} + 2(\sqrt{3}r_{100} - 2r_{111})\sigma_{111}}{r_{111}^2 - (\sqrt{3}r_{111} - r_{100})^2} V_m$
Type B ($2/\sqrt{3} \le r_{111}/r_{100} \le \sqrt{3}$)	$\frac{2(3\sqrt{3}r_{111} - 7r_{100})\sigma_{100} + 6(\sqrt{3}r_{100} - r_{111})\sigma_{111}}{2r_{100}^2 - 3(\sqrt{3}r_{100} - r_{111})^2} V_m$	$\frac{2\sqrt{3}\sigma_{100} - 2\sigma_{111}}{\sqrt{3}r_{100} - r_{111}} V_m$

The chemical potential of solute in equlibrium with a {100} face, μ_L^{100}, is given by:

$$\mu_L^{100} = \mu_{100} + \mu_\infty \quad , \tag{24}$$

where μ_∞ is the chemical potential of a particle of infinite dimensions. On the other hand, μ_L^{100} and μ_∞ are related to the activities of the electrolyte or the solubility products as:

$$\mu_L^{100} = \mu^\circ + RT\ln K_{sp}^{100} \tag{25}$$

$$\mu_\infty = \mu^\circ + RT\ln K_{sp}^{\infty} \quad , \tag{26}$$

where μ° is the standard chemical potential, K_{sp}^{100} is the solubility product of a {100} face of the tetradecahedral particle, K_{sp}^{∞} is the solubility product of the infinite-sized particle, R is the gas constant and T is the absolute temperature. Similar relationships are obtained for a {111} face as well.

Thus, K_{sp}^{100} and K_{sp}^{100} are expressed as functions of μ_{100} and μ_{111} respectively:

$$\left.\begin{aligned} K_{sp}^{100} &= K_{sp}^{\infty}\exp(\mu_{100}/RT) \\ K_{sp}^{111} &= K_{sp}^{\infty}\exp(\mu_{111}/RT) \end{aligned}\right\} , \qquad (27)$$

Eq. 27 means that the solubility or the solubility product of each facet of the tetradecahedral microcrystal can be calculated if the shape, size and specific surface energies of the {100} and {111} faces are known. The relations of Eq. 27 can be applied to non-equilibrium forms as well as equilibrium ones, as has been verified for tabular grains of AgBr (ref. 163).

B. Stable forms

1. Equilibrium forms. If both the {100} and {111} faces coexist within a tetrdecahedron in equlibrium with a common solution, SCP's of the {100} and {111} faces are equal:

$$\mu_{100} = \mu_{111} \quad . \qquad (28)$$

Applying this relation to μ_{100} and μ_{111} in Table 1, it follows for both types A and B that:

$$\frac{r_{111}}{r_{100}} = \frac{\sigma_{111}}{\sigma_{100}} , \qquad (29)$$

which conforms to the Wulff-theorem in Eq. 21. In this case, α ($\equiv \sigma_{111}/\sigma_{100}$) must be in the range of $1/\sqrt{3} < \alpha < \sqrt{3}$ due to the geometric restriction of a tetradecahedron: $1/\sqrt{3} < p < \sqrt{3}$ ($p \equiv r_{111}/r_{100}$).

If $\alpha \leq 1/\sqrt{3}$, $\mu_{111} > \mu_{100}$ always holds for $1/\sqrt{3} < p < \sqrt{3}$ from Table 1. Thus, the {100} faces continue to grow with the dissolution of the {111} faces until the {100} faces disappear to form a perfect octahedron ($p = 1/\sqrt{3}$).

If $\alpha \geq \sqrt{3}$, $\mu_{111} < \mu_{100}$ holds for $1/\sqrt{3} < p < \sqrt{3}$. Thus, the {111} faces grow at the expense of the {100} faces until the {111} faces vanish to form a perfect cube ($p = \sqrt{3}$). Although the last two cases do not satisfy the Wulff formula, they comply with the Gibbs principle of the equilibrium form.

The change of the SCP's of the {100} and {111} faces is shown as a function of p in Fig. 14 for a constant particle volume where f is the surface chemical potential relative to μ_{100} of a cube of the same volume. Table 2 summarizes the SCP's of the equilibrium forms in the respective ranges of $\alpha(\equiv \sigma_{111}/\sigma_{100})$.

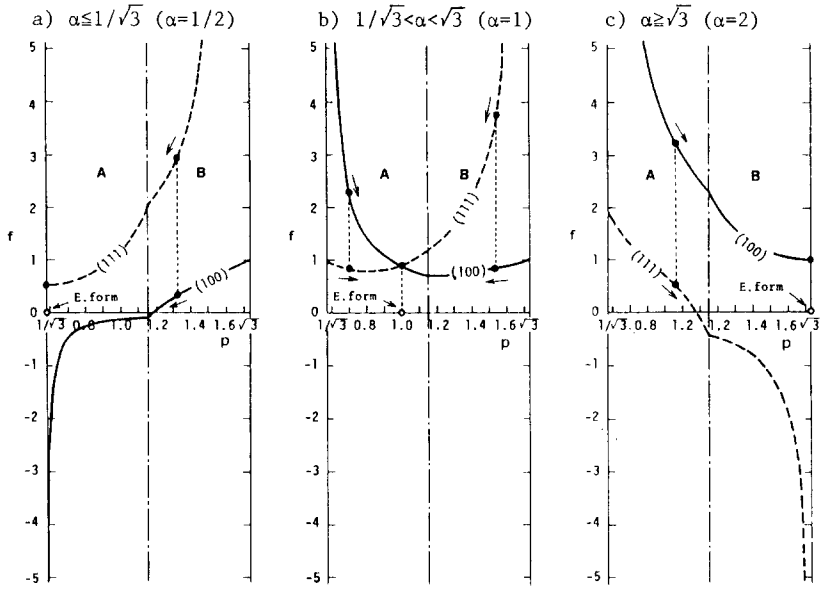

Fig. 14. Surface chemical potentials of {100} and {111} faces of a tetradecahedral microcrystal for the three ranges of α. The arrows indicate the directions of driving force (ref. 162).

TABLE 2

Relationships between the equilibrium form and the surface chemical potential for the respective ranges of $\sigma_{111}/\sigma_{100}$ (ref. 162).

$\sigma_{111}/\sigma_{100}$	r_{111}/r_{100}	Equilibrium forms	Surface chemical potentials of equilibrium forms	
			μ_{100}	μ_{111}
$\sigma_{111}/\sigma_{100} \leq 1/\sqrt{3}$	$1/\sqrt{3}$	Oct.	$-\infty$	$2\sigma_{111}V_m/r_{111}$
$1/\sqrt{3} < \sigma_{111}/\sigma_{100} < \sqrt{3}$	$\sigma_{111}/\sigma_{100}$	Tetradec.	$2\sigma_{100}V_m/r_{100}$	$2\sigma_{111}V_m/r_{111}$
$\sigma_{111}/\sigma_{100} \geq \sqrt{3}$	$\sqrt{3}$	Cub.	$2\sigma_{100}V_m/r_{100}$	$-\infty$

2. Steady forms

a) Reaction-controlled growth. A microcrystal which is grown under supersaturation is expected to assume a balanced steady form because the growth rate of one kind of facets which at first grow faster than the other will soon be limited by the lowered supersaturation due to the higher solubility of their own projected faces with a longer central distance (see Fig. 14b). Thus, the "steady form" is defined as a kind of growth form dynamically stabilized by the steady growth under a supersaturation.

If a particle grows by a steady reaction control, it is necessary for the derivative of p with regard to time to be zero:

$$\dot{p} = 0 \ . \tag{30}$$

Meanwhile, $\dot{p}$ is given by

$$\dot{p} = -\frac{\dot{r}_{100}}{r_{100}}\left(p - \frac{\dot{r}_{111}}{\dot{r}_{100}}\right) \ . \tag{31}$$

Thus, it follows that:

$$p = \frac{\dot{r}_{111}}{\dot{r}_{100}} \ . \tag{32}$$

Designating the steady state with an asterisk, Eq. 32 can be written as:

$$p^* = \frac{k_{111}(C-C^*_{111})}{k_{100}(C-C^*_{100})} \ , \tag{33}$$

where k_{111} and k_{100} are the growth rate constants of the {111} and the {100} faces, respectively, on the assumption of reaction-controlled growth, C is the solute concentration in the bulk solution and C^*_{11} and C^*_{00} are the solubilities of the {111} and {100} faces of the steady form, respectively. The solutions of Eq. 33 for p* are graphically given by intersections of the following two functions of p:

$$y_1 = \frac{k_{100}}{k_{111}}p \ ; \tag{34}$$

$$y_2 = \frac{C-C_{111}}{C-C_{100}} \ . \tag{35}$$

Eq. 35 is rewritten from Eq. 27 as:

$$y_2 = \frac{C/C_\infty - \exp(\mu_{111}/RT)}{C/C_\infty - \exp(\mu_{100}/RT)} \ , \tag{36}$$

where C_∞ is the solubility of an infinite-sized particle.

Examples of the graphic determination of p* are shown in Fig. 15 according to the range of α where it is assumed that $C/C_\infty = 1.3$, $\nu = 1\ \mu m^3$ and $\sigma_{100} = 150\ erg/cm^2$.

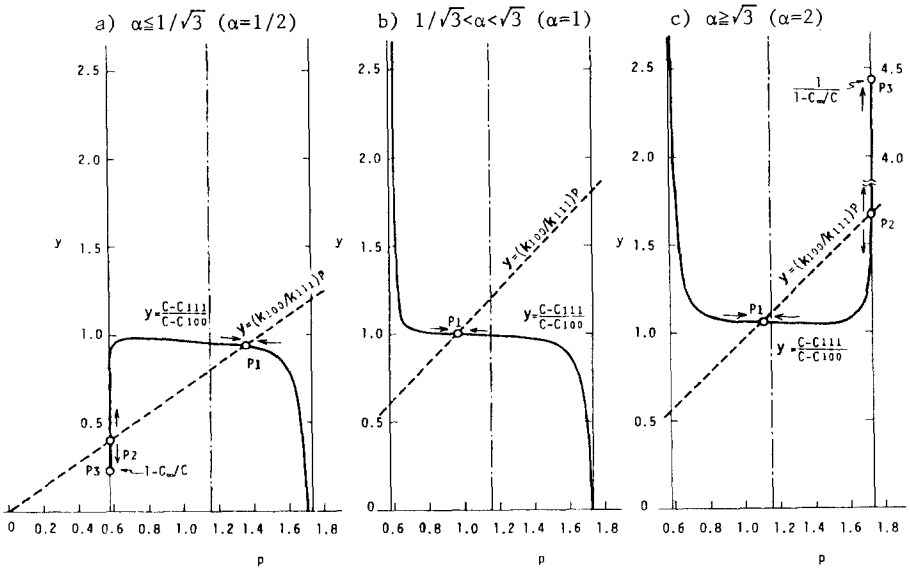

Fig. 15. Graphic determination of the steady forms for the three ranges of α. Arrows indicate the directions of driving force (ref. 162).

In Fig. 15, the intersections of P_1 and P_2 as well as the terminal point P_3 fulfill the necessary condition, $\dot{p} = 0$. However, the following condition is further required for the steady form to be stable:

$$\frac{d\dot{p}}{dp} < 0 \quad . \tag{37}$$

Thus, the p values at P_1 and P_3 are eligible for the steady forms which suffice the entire requirements.

For $1/\sqrt{3} < \alpha < \sqrt{3}$, all particles in a system stay at a single p^* of P_1 during their growth (Fig. 15b) and p^* is approximately given as:

$$\left.\begin{aligned} p^* &= \frac{1}{\sqrt{3}} \quad \text{for} \quad \frac{k_{111}}{k_{100}} \leqq \frac{1}{\sqrt{3}} \quad , \\ &= \frac{k_{11}}{k_{10}} \quad \text{for} \quad \frac{1}{\sqrt{3}} < \frac{k_{111}}{k_{100}} < \sqrt{3} \quad , \\ &= \sqrt{3} \quad \text{for} \quad \frac{k_{111}}{k_{100}} \geqq \sqrt{3} \quad . \end{aligned}\right\} \tag{38}$$

On the other hand, for $\alpha \leqq 1/\sqrt{3}$ and $\alpha \geqq \sqrt{3}$, two values of p^* at P_1 and P_3 are feasible in some cases ($1/\sqrt{3} < k_{111}/k_{100} < \sqrt{3}$) (Fig. 15a,c): p^* of P_1 is approximately given as k_{111}/k_{100}, whereas p^* of P_3 is equal to $1/\sqrt{3}$ (octahedron) for $\alpha \leqq 1/\sqrt{3}$ or $\sqrt{3}$ (cube) for $\alpha \geqq \sqrt{3}$; i.e., particles of two different shapes may coexist in a system when k_{111}/k_{100} falls in $1/\sqrt{3} < k_{111}/k_{100} < \sqrt{3}$. Thus, in this case, the system is not perfectly uniform.

Although experimental evidence for such a deduction has never yet been given, it is possible that the separation in morphology takes place in a real system by the above mechanism.

Except for these special cases, p* of the steady form can be written by Eq. 38 for reaction-controlled growth. This conclusion can be extended to a general polyhedral particle which possesses different kinds of faces as a steady form; i.e.:

$$r_1 : r_2 : r_3 \text{ ---: } r_i \text{ ---: } r_n = k_1 : k_2 : k_3 \text{ ---: } k_i \text{ ---: } k_n \quad , \tag{39}$$

where r_i and k_i are the central distance to and the growth rate constant of the faces of the ith kind, respectively.

b) Diffusion-controlled growth. If a polyhedral microcrystal grows by an ideal diffusion control where both growth and dissolution at the interface are quick enough as compared to the diffusion of solute toward the interface, the concentration of solute at the interface must be virtually in equilibrium with each face of the microcrystal. Accordingly, the steady form of a polyhedral microcrystal which grows by ideal diffusion control is equal to the equilibrium form. In other words, Curie's hypothesis referred to earlier in this chapter is valid for a colloidal microcrystal which grows by the ideal diffusion control mechanism. This model is illustrated in Fig. 16 for the case of a tetradecahedral particle in $1/\sqrt{3} < \alpha < \sqrt{3}$.

Therefore, p* for diffusion-controlled growth is written as:

$$\begin{aligned} p^* &= \frac{1}{\sqrt{3}} && \text{for } \alpha \leq \frac{1}{\sqrt{3}} \quad , \\ &= \frac{\sigma_{111}}{\alpha_{100}} && \text{for } \frac{1}{\sqrt{3}} < \alpha < \sqrt{3} \quad , \\ &= \sqrt{3} && \text{for } \alpha \geq \sqrt{3} \ . \end{aligned} \tag{40}$$

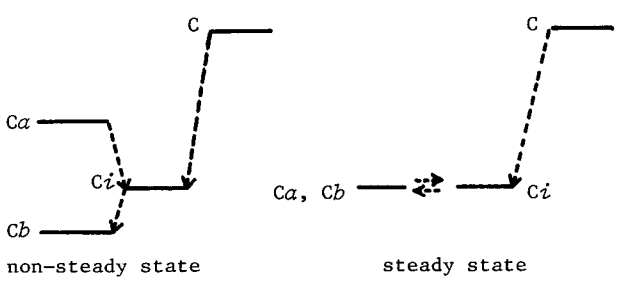

Fig. 16. Concentration levels of solute for the ideal diffusion-controlled growth of a tetradecahedral particle in a non-steady state and the steady state for $1/\sqrt{3} < \alpha < \sqrt{3}$. The two kinds of faces are designated by *a* and *b*. The arrows indicate the directions of mass transfer of solute (ref. 94).

Needless to say, the steady form of a general polyhedral particle bound by several kinds of faces after the ideal diffusion-controlled growth can be written as:

$$r_1 : r_2 : r_3 \text{ ---: } r_i \text{ ---: } r_n = \sigma_1 : \sigma_2 : \sigma_3 : \text{ ---: } \sigma_i \text{ ---: } \sigma_n \ , \qquad (41)$$

where r_i and σ_i are the central distance to and the specific surface energy of the faces of the ith kind, respectively

C. Examples of the equilibrium form and the steady form.

As typical examples of both stable forms and their correlation, the experimental results on monodispersed microcrystals of silver bromide may be appropriate to review.

The equilibrium form is attainable only in a monodisperse colloidal system since otherwise it is impossible for every microcrystal to arrive at equilibrium with solute due to Ostwald ripening (ref. 93,93). Fig. 17 is an example of the equilibrium form as a function of pBr reached from monodispersed cubic and octahedral silver bromide microcrystals by aging in 0.5M ammoniacal media at 50°C (ref. 162). The ratio of r_{111}/r_{100} was determined by measuring the respective surface areas of the {111} and the {100} faces by dye-adsorption method. In this case, since the r_{111}/r_{100} ratio falls in $1/\sqrt{3} < r_{111}/r_{100} < \sqrt{3}$, the equilibrium form satisfies the relation of $r_{111}/r_{100} = \sigma_{111}/\sigma_{100}$. Since adsorption of any species results in the reduction of specific surface energy (ref. 148), the values of σ_{111}, σ_{100} and $\sigma_{111}/\sigma_{100}$ are altered as functions of excess bromide or pBr ($\equiv -\log [Br^-]$) by adsorption of bromide to the respective faces.

On the other hand, the ratio of r_{111}/r_{100} can be varied in open systems as well by the change of excess concentration of bromide or pBr. The open system for a silver bromide dispersion consists of the concurrent introduction of silver nitrate and halide solutions into a well stirred gelatin solution. Normally, the pBr is electronically regulated throughout the precipitation by monitoring the activity of silver ions with a silver electrode (ref. 164). The alteration of $\dot{r}_{111}/\dot{r}_{100}$ with pBr has been explained in terms of the change in peripheral surface energy of the two-dimensional nuclei on the respective faces by adsorption of bromide (ref. 12). This is essentially based on the Stranski theory (ref. 151) which predicts the reduction of the growth rate of {111} faces and the promotion of the growth of {100} faces by adsorption of solute species. Thus, the microcrystals obtained assume a typical steady form.

Fig. 18 shows the electron micrographs of silver bromide particles in steady form obtained in 0.5M ammoniacal solutions of an open system at 50°C with the variation of pBr (ref. 162). In this case, the particles grow by

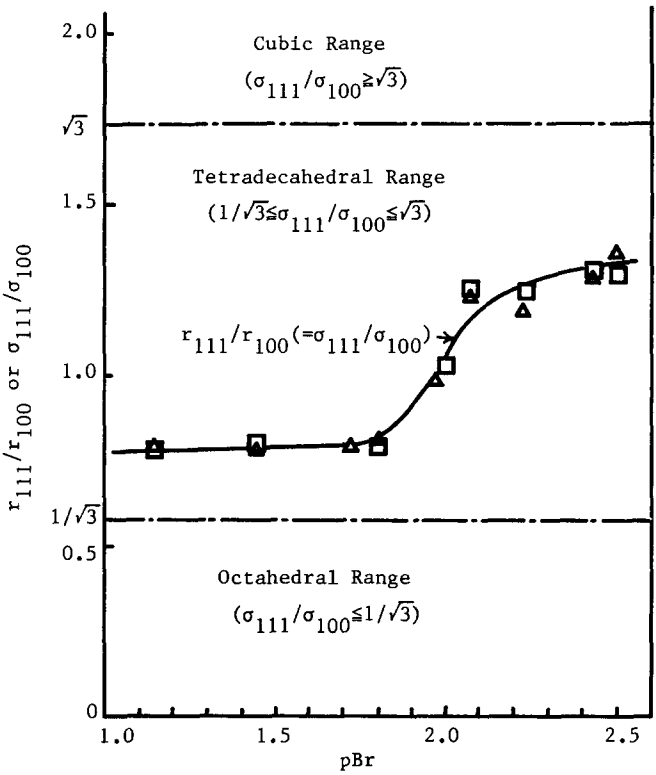

Fig. 17. Ratio of r_{111}/r_{100} or $\sigma_{111}/\sigma_{100}$ of the equilibrium form of AgBr as a function of pBr in an ammoniacal solution (ref. 162).

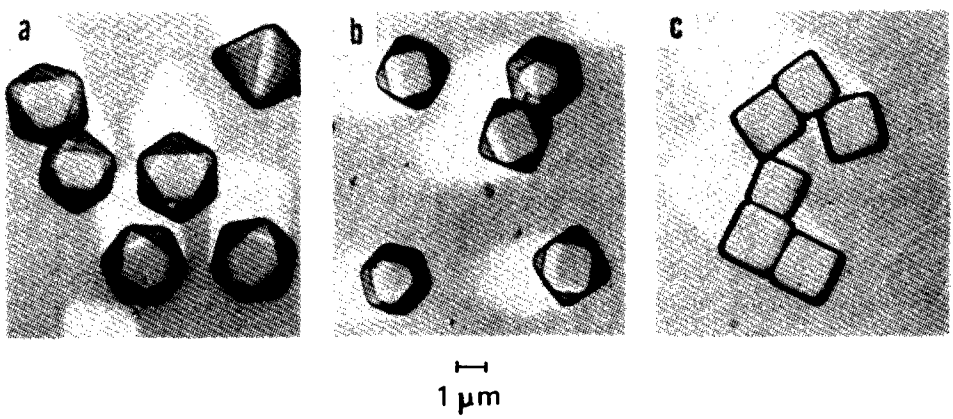

Fig. 18. Electron micrographs of monodispersed AgBr microcrystals prepared by simultaneous addition of $AgNO_3$ and KBr solutions at constant pBr in the presence of ammonia: (a) pBr = 1.40; (b) 1.90; (c) 2.30 (ref. 162).
reaction control due to adsorption of ammonia on their surfaces so that the

shape is determined by the ratio of $\dot{r}_{111}/\dot{r}_{100}$; e.g., $r_{111}/r_{100} = \dot{r}_{111}/\dot{r}_{100} \cong k_{111}/k_{100}$ for $1/\sqrt{3} < \dot{r}_{111}/\dot{r}_{100} < \sqrt{3}$ (ref. 162). The result is shown in Fig. 19 as a function of pBr, where the r_{111}/r_{100} ratio of the equilibrium form is superimposed for comparison. Here, $\dot{r}_{111}$ and $\dot{r}_{100}$ were determined by measuring the initial growth rates of octahedral and cubic particles, respectively.

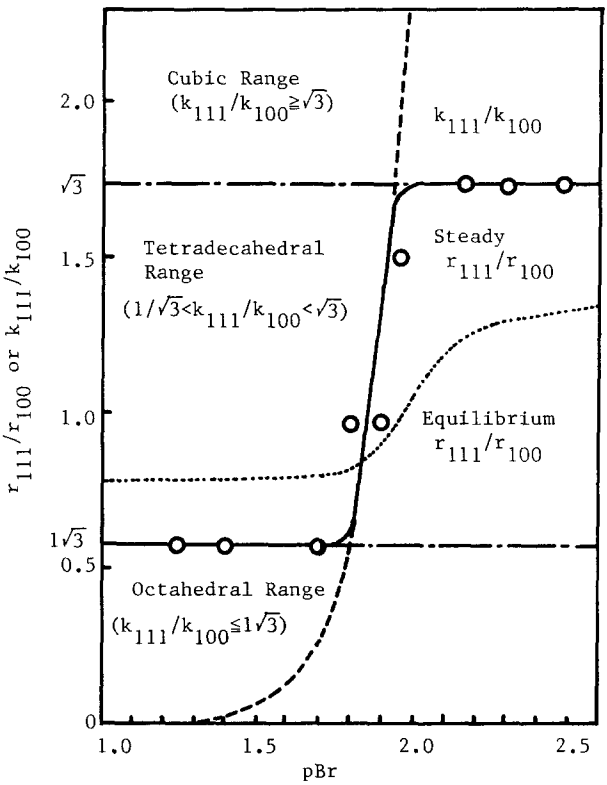

Fig. 19. Ratio of k_{111}/k_{100} or r_{111}/r_{100} for the reaction-controlled steady form as a function of pBr. The ratio of r_{111}/r_{100} for the equilibrium form is superimposed for comparison (ref. 162).

In the absence of ammonia, the r_{111}/r_{100} ratio of the steady form fails to agree with $\dot{r}_{111}/\dot{r}_{100} (= K_{111}/K_{100})$ as shown in Fig. 20 (ref. 94). This is because both the {111} and {100} faces grow by diffusion control in the pBr range from 2.6 to 3.5 as a result of being free from adsorption of ammonia. Thus, a tetradecahedral particle grown in this pBr range is considered to assume the equilibrium form as its steady form.

On the other hand, monodispersed cubic particles of AgCl are known to grow by diffusion control in open systems, probably for any pCl (ref. 165). Hence, the steady form of AgCl appears to coincide with the equilibrium form with $\sigma_{111}/\sigma_{100} \geq \sqrt{3}$.

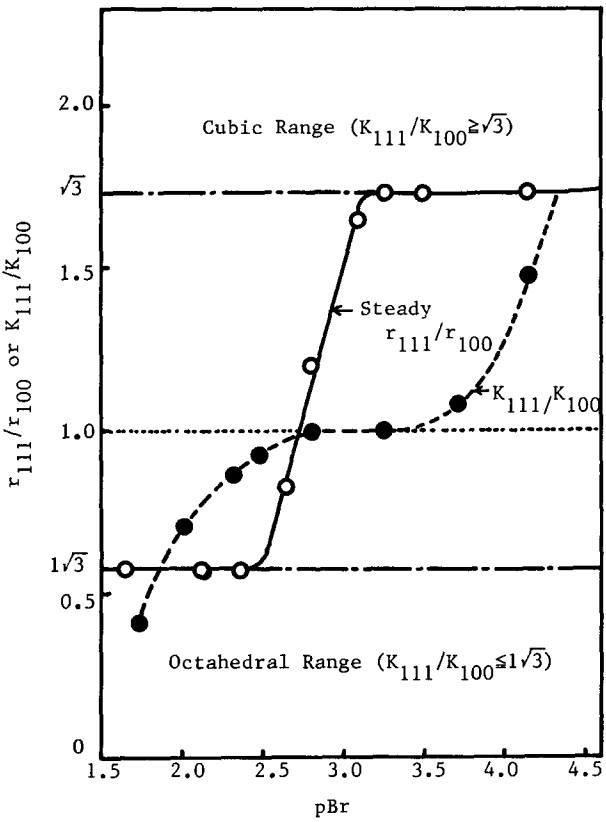

Fig. 20. Ratio of K_{111}/K_{100} or r_{111}/r_{100} for the diffusion-controlled steady form as a function of pBr (ref. 94).

V. CONCLUDING REMARKS

Although studies on monodispersed particle formation have been so markedly advanced by the strenuous efforts of numerous researchers that we are now getting away from the sheer trial-and-error stage, establishing a new monodipserse system still appears to be an arduous task with a flavor of art. In this sense, there is no royal road to the goal, despite the growing demand for such uniform systems. Nevertheless, the author believes that there are some common rules behind the individual peculiarities and that it is well timed to present his personal outlook on this fascinating field in view of the current trends.

Thus, in this review, the underlying principles for the preparation of well defined monodispersed colloids and the formation of characteristic crystal habit have been considered on a comprehensive analysis of the existing examples from theoretical and empirical points of view. The readers must have found that all systems basically comply with the proposed general rules.

However, the guidelines set forth in this article are far from satisfactory to reach ideally uniform systems with little experimental effort; but, hopefully, they might be of some help to the people who are actually involved in the development of new monodisperse systems or generally interested in the mechanism of colloidal particle formation.

VI. ACKNOWLEDGEMENT

The author wishes to gratefully acknowledge Prof. E. Matijević in Clarkson University for encouraging this review with the kindly offer of his latest publications.

VII. REFERENCES

1 E. Matijević, Prog. Colloid and Polymer Sci., 61(1976)24.
2 E. Matijević, "Trends in Electrochemistry," J.O'M. Bockris et al., ed., Plenum, p. 177, 1977.
3 E. Matijević, Pure and Appl. Chem., 50(1978)1193.
4 E. Matijević, Corrosion, 35(1979)264.
5 E. Matijević, Pure and Appl. Chem., 52(1980)1179.
6 E. Matijević, Acc. Chem. Res., 14(1981)22.
7 E. Matijević, Ann. Rev. Mater. Sci., 15(1985)483.
8 E. Matijević, Langmuir, 2(1986)12.
9 C.R. Berry, J. Opt. Soc. Am., 52(1961)888.
10 C.R. Berry. S.J. Marino and C.F. Oster, Jr., Phot. Sci. Eng., 5(1961)332.
11 C.R. Berry and D.C. Skillman, Phot. Sci. Eng., 6(1962)159.
12 E. Moisar and E. Klein, Ber. Bunsenges. Phys. Chem., 67(1963)949.
13 J.Th.G. Overbeek, Adv. Colloid Interface Sci., 15(1982)251.
14 T. Sugimoto, Hyomen, 22(1984)177.
15 V.K. LaMer and R.H. Dinegar, J. Am. Chem. Soc., 72(1950)4847.
16 R. Zsigmondy, Z. Anorg. Allgem. Chem., 99(1917)105.
17 T. Sugimoto and G. Yamaguchi, J. Crystal Growth, 34(1976)253.
18 T. Sugimoto and E. Matijević, J. Inorg. Nucl. Chem., 41(1979)165.
19 T. Sugimoto and E. Matijević, J. Colloid Interface Sci., 74(1980)227.
20 F.T. Hesselink, A. Vrij and J.Th.G. Overbeek, J. Phys. Chem., 75(1971)2094.
21 H. Thiele and H.S. Van Levern, J. Colloid Sci., 20(1965)679.
22 T. Sugimoto, AIChE Journal, 24(1978)1125.
23 A.E. Nielsen, "Kinetics of Precipitation", Pergamon, New York, 1964.
24 J.S. Wey and R.W. Strong, Phot. Sci. Eng., 21(1977)248.
25 R. Zsigmondy, Z. Physik. Chem., 56(1906)65,77.
26 K. Takiyama, Bull. Chem. Soc. Japan, 31(1958)944.
27 J. Turkevick, R.C. Stevenson and J. Hillier, Discuss. Faraday Soc., 11(1959)55.
28 A. Watillon and J. Dauchot, J. Colloid Interface Sci., 27(1968)507.
29 A. Watillon, F. van Grunderbeeck and M. Hautecler, Bull. Soc. Chim. Belges., 67(1958)5.
30 R.S. Sapieszko and E. Matijević, Corrosion, 36(1980)522.
31 R.H. Ottewill and R.F. Woodbridge, J. Phot. Sci., 13(1965)98.
32 P. McFadyen and E. Matijević, J. Colloid Interface Sci., 44(1973)95.
33 G. Chiu and E.J. Meehan, J. Colloid Interface Sci., 62(1977)1.
34 I. Joekes, F. Galembeck, H.S. Santos and M. Jafelicci, Jr., J. Collolid Interface Sci., 84(1981)278.
35 R. Ginell, A.M. Ginell and P.E. Spoerri, J. Colloid Interface Sci., 2(1947)521.
36 M.J. Herak, M.M. Herak, B. Tezak and J. Kratohvil, Arhiv. Kem., 27(1955)117.
37 M.J. Herak, J. Kratohvil, M.M. Herak and M. Wrischer, Croat. Chem. Acta, 30(1958)221.
38 R.B. Wilhelmy and E. Matijević, Diss. Abstr. Int., B43(1983)2920.

39 E.P. Katsanis and E. Matijević, Colloid Surf., 5(1982)43.
40 G. Chiu and E.J. Meehan, J. Colloid Interface Sci., 49(1974)160.
41 G. Chiu, J. Colloid Interface Sci., 62(177)193.
42 G. Chiu, J. Colloid Interface Sci., 83(1981)309.
43 V.K. LaMer and M.D. Barnes, J. Colloid Sci., 1(1946)71.
44 I. Johnson and V.K. LaMer, J. Am. Chem. Soc., 69(1947)1184.
45 M. Kerker, E. Davy, G.L. Cohen, J.P. Kratohvil and E. Matijevic, J. Phys. Chem., 67(1963)2105.
46 M. Kerker, W.A. Farone and W.F. Espenscheid, J. Colloid and Interface Sci., 21(1966)459.
47 M. Kerker, W.A. Farone and R.T. Jacobsen, J. Opt. Soc. Amer., 56(1966)56.
48 K. Takiyama, Bull. Chem. Soc. Japan, 31(1958)950.
49 E. Matijević and D.W. Wilhelmy, J. Colloid Interface Sci., 86(1982)476.
50 D.M. Wilhelmy and E. Matijević, J. Chem. Soc., Faraday Trans., 80(1984)563.
51 D.M. Wilhelmy and E. Matijević, Colloid Surf., 16(1985)1.
52 J. Gobet and E. Matijević, J. Colloid Interface Sci., 100(1984)555.
53 M. Haruta, J. Lamaitre, F. Delannay and B. Delmon, J. Colloid Interface Sci., 101(1984)59.
54 A. Janeković and E. Matijević, J. Colloid Interface Sci., 103(1985)436.
55 R.S. Sapieszko and E. Matijević, J. Colloid Interface Sci., 74(1980)405.
56 R.H. Ottewill and R.F. Woodbridge, J. Colloid Sci., 16(1961)581.
57 W. Stöber, A. Fink and E. Bohn, J. Colloid Interface Sci., 26(1968)62.
58 C.A. Barringer and H.K. Bowen, J. Am. Ceram. Soc., 65(1982)C-199.
59 T. Ikemoto, K. Umematsu, N. Mizutani and M. Kato, Yogyo-Kyokai-Shi, 93(1985)261.
60 J.H. Jean and T.A. Ring, Langmuir, 2(1986)251.
61 E.S. Tormey, R.L. Pober, H.K. Bowen and P.D. Calvert, "Advances in Ceramics", J.A. Manges et al., eds., American Ceramics Society Press, Columbus, Vol. 9, p. 140, 1984.
62 B. Fegley, Jr. and E.A. Barringer, "Better Ceramics Through Chemistry, Elsevier, p. 187, 1984.
63 T. Ikemoto, N. Mizutani, M. Kato and Y. Mitarai, Yogyo-Kyokai-Shi, 93(1985)585.
64 R. Demchak and E. Matijević, J. Colloid Interface Sci., 31(1969)257.
65 R. Brace and E. Matijević, J. Inorg. Nucl. Chem., 35(1973)3691.
66 D.L. Catone and E. Matijević, J. Colloid Interface Sci., 48(1974)291.
67 W.B. Scott and E. Matijević, J. Colloid Interface Sci., 66(1978)447.
68 E. Matijević and P. Scheiner, J. Colloid Interface Sci., 63(1978)509.
69 S. Hamada and E. Matijević, J. Chem. Soc. Faraday Trans. I, 78(1982)2147.
70 S. Hamada, T. Hanami and Y. Kudo, J. Chem. Soc. Japan, 6(1984)1065.
71 M. Ozaki, S. Kratohvil and E. Matijević, J. Colloid Interface Sci., 102(1984)146.
72 S. Hamada, S. Niizeki and Y. Kudo, Bull. Chem. Soc. Japan, 59(1986)3443.
73 E. Matijević, R.S. Sapieszko and J.B. Melville, J. Colloid Interface Sci., 50(1975)567.
74 E. Matijević, M. Budnik and L. Meites, J. Colloid Interface Sci., 61(1977)302.
75 N.B. Milic and E. Matijević, J. Colloid Interface Sci., 85(1982)306.
76 S. Hamada, K. Bando and Y. Kudo, J. Chem. Soc. Japan, 6(1984)1068.
77 S. Hamada, K. Bando and Y. Kudo, Bull. Chem. Soc. Japan, 59(1986)2063.
78 D.H. Buss, G. Schaumberg and O. Glemser, Angew. Chem., 97(1985)1050.
79 M.A. Blesa, A.J.G. Maroto, S.I. Passaggio, N.E. Figliolia and G. Rigotti, J. Mater. Sci., 20(1985)4601.
80 J.H.L. Watson, W. Heller and W. Wojtowicz, J. Chem. Phys., 16(1948)997.
81 J.H.L. Watson, R.R. Cardell, Jr., and W. Heller, J. Phys. Chem., 66(1962)1757.
82 M. Ozaki and E. Matijević, J. Colloid Interface Sci., 107(1985)199.
83 R.S. Sapieszko, R.C. Patel and E. Matijević, J. Phys. Chem., 81(1977)1061.
84 E. Matijević, A.D. Lindsey, S. Kratohvil, M.E. Jones, R.I. Larson and N.W. Cayey, J. Colloid Interface Sci., 36(1971)273.
85 A. Bell and E. Matijević, J. Inorg. Nucl. Chem., 37(1975)907.
86 S.S. Singh, Can. J. Soil Sci., 499(1969)383.

87 N. Kallay, I. Fischer and E. Matijević, Colloid Surf., 13(1985)145.
88 K. Bridger, R.D. Patel and E. Matijević, J. Inorg. Nucl. Chem., 43(1981)1011.
89 A.E. Reganzzoni and E. Matijević, Corrosion, 38(1982)212.
90 H. Tamura and E. Matijević, J. Colloid Interface Sci., 90(1982)100.
91 A.E. Reganzzoni and E. Matijević, Colloid Surf., 6(1983)189.
92 I.M. Lifshitz and V.V. Slyozov, J. Phys. Chem. Solids, 19(1961)35.
93 C. Wagner, Z. Elektrochem., 65(1961)581.
94 T. Sugimoto, J. Colloid Interface Sci., 93(1983)461.
95 J.D. Lewis, U.S. Patent 4,067,739 (1978).
96 M. Saito, U.S. Patent 4,242,445 (1980).
97 E.B. Bradford and J. W. Vanderhoff, J. Appl. Phys., 26(1955)864.
98 E.B. Bradford, J.W. Vanderhoff and T. Alfrey, Jr., J. Colloid Sci., 11(1956)135.
99 W.B. Dandliker, J.Am. Chem. Soc., 72(1950)5110.
100 M. Kerker, "The Scattering of Light and Other Electromagnetic Radiation", Academic Press, New York, 1969.
101 J.W. Vanderhoff, Pure Appl. Chem., 52(1980)1263.
102 A.A. Kamel, M.S. El-Aasser and J.W. Vanderhoff, J. Disp. Sci. Tech., 2(1981)183.
103 W.D. Harkins, J. Am. Chem. Soc., 69(1947)1428.
104 W.V. Smith and R.H. Ewart, J. Chem. Phys., 16(1948)592.
105 J.W. Vanderhoff, J.F. Vitkuske, E.B. Bradford and T. Alfrey, J. Polym. Sci., 20(1956)225.
106 R.H. Ottewill and J.N. Shaw, Kolloid Z.-Z.Polylm., 215(1967)161.
107 J.W. Goodwin, J. Hearn, C. C. Ho and R.H. Ottewill, Colloid and Polymer Sci., 252(1974)464.
108 S. Yamazaki, Kobunshi Ronbunshu, 33(1976)559.
109 J.W. Goodwin, R.H. Ottewill and R. Pelton, Colloid and Polymer Sci, 257(1979)61.
110 S. Yamazaki, M. Hamashima and Y. Ishigami, Kobunshi Ronbunshu, 33(1976)549.
111 H. Kawaguchi, Y. Sugi and Y. Ohtsuka, "Emulsion Polymers and Emulsion Polymerization", D.R. Bassett and A.E. Hamielec, Eds., Am. Chem. Soc. Symposium Series, Washington, D.C., p. 145, 1981.
112 H. Kawaguchi, M. Nakamura, M. Yanagisawa, F. Hishino and Y. Ohtusuka, Makromol. Chem. Rapid Commun., 6(1985)315.
113 J.W. Vanderhoff, E.B. Bradford and H.L. Tarkowski, J. Polym. Sci., 50(1961)265.
114 J. Ugelstad, P.C. Mork, K.H. Kaggerud, T. Ellingsen and A. Berge, Adv. Colloid Interface Sci., 13(1980)101.
115 A.T. Skjeltorp, J. Ugelstad and T. Ellingsen, J. Colloid Interface Sci., 113(1986)577.
116 P. Pendleton, B. Vincent and M.L. Hair, J. Colloid Interface Sci., 80(1981)512.
117 P.K. Isaacs and A. Trafimow, U.S. Patent 3,033,812 (1962).
118 M. Boutonnet, J. Kizling, P. Stenius and G. Maire, Colloid Surf., 5(1982)209.
119 J.B. Nagy, A. Gourgue and E.G. Deroune, "Third International Symposium on Scientific Bases for the Preparation of Heterogeneous Catalysts", Lowan-la-Neuve, Sept. 1982, Elsevier, Amstrdam, 1982.
120 N. Lufimpadio, J.B. Nagy and E.G. Deroune, "Proceedings of the Symposium on Surfactants in Solution", Lund, Sweden, June 1982.
121 K. Kurihara, J. Kizling, P. Stenius and J.H. Fendler, J. Am. Chem. Soc., 105(1983)2574.
122 M. Gobe, K. Kon-no, K. Kandori and A. Kitahara, J. Colloid Interface Sci., 93(1983)293.
123 M. Dvolaitzky, R. Ober, C. Taupin, R. Anthore, X. Auvray and C. Petipas, J. Disp. Sci. Tech., 4(1983)29.
124 K. Kon-no, M. Koide and A. Kitahara, J. Chem. Soc. Japan, 6(1984)815.
125 N. Shizuka, M. Yanagi, K. Kon-no and A. Kitahara, "Proceedings of the 37th Symposium on Colloid and Interface Chemistry", Morioka, Japan, p. 360, 1984.

126 K. Kandori, N. Shizuka, K. Kon-no and A. Kitahara, submitted to J. Dispersion Sci. Tech.
127 M. Yanagi, Y. Asano, K. Kandori, K. Kon-no and A. Kitahara, "1986 Shikizai Technical Conference", Osaka, Japan, p. 86, 1986.
128 S.S. Atik and J.K. Thomas, J. Am. Chem. Soc., 103(1981)4279.
129 P. Lianos, J. Phys. Chem., 86(1982)1935.
130 Y.S. Leong, G. Riess and F. Candau, J. Chim. Phys., 78(1981)279.
131 Y.S. Leong and F. Candau, J. Phys. Chem., 86(1982)2269.
132 F. Candau, Y.S. Leong, G. Pouyet and S. Candau, J. Colloid Interface Sci., 101(1984)167.
133 F. Candau, Y.S. Leong and R.M. Fitch, J. Polym. Sci.: Polym. Chem. Edn., 23(1985)193.
134 M. Gobe, K. Kon-no and A. Kitahara, "The Proceedings of the 35th Symposium on Colloid and Interface Chemistry", Kiriu, Japan, p. 36, 1982.
135 F. Candau, Z. Zekhnini, F. Heatley and E. Franta, Colloid Polym. Sci., 264(1986)676.
136 M. Visca and E. Matijević, J. Colloid Interface Sci., 68(19769)308.
137 B.J. Ingebrethsen and E. Matijević, J. Aerosol Sci., 11(1980)271.
138 B.J. Ingebrethsen, E. Matijević and R.E. Partch, J. Colloid Interface Sci., 95(1983)228.
139 R.E. Partch, E. Matijević, A.W. Hodgson and B.F. Aiken, J. Polym. Sci., Polym. Chem. Edn., 21(1983)961.
140 K. Nakamura, R.E. Partch and E. Matijević, J. Colloid Interface Sci., 99(1984)118.
141 R.E. Partch, K. Nakamura, K.J. Wolfe and E. Matijević, J. Colloid Interface Sci., 105(1985)560.
142 D. Sinclair and V.K. LaMer, Chem. Rev., 44(1949)245.
143 V.K. LaMer, E.C.Y. Inn and I.B. Wilson, J. Colloid Sci., 5(1950)471.
144 E. Matijević, S. Kitani and M. Kerker, J. Colloid Sci., 19(1964)223.
145 G. Nicolaon, D.D. Cooke, M. Kerker and E. Matijević, J. Colloid Interface Sci., 34(1970)534.
146 G. Kasper and A. Berner, Staub-Reinhalt. Luft, 38(1978)183.
147 C. Hillenbrand and J. Porstendoerfer, Staub-Reinhalt. Luft, 38(1978)52.
148 C.W. Bunn, Diss. Faraday Soc., 5(1949)132.
149 H.E. Buckley, "Crystal Growth", John Wiley and Sons, New York, 1951.
150 R. Kern, Compt. Rend., 236(1953)830.
151 O. Knack and J.N. Stranski, Z. Elektrochem., 60(1956)816.
152 C.R. Berry, Phot. Sci. Eng., 18(1974)4.
153 W. Markocki and A. Zaleski, Phot. Sci. Eng., 176(1973)289.
154 S. Nishiyama, German Patent (O.L.S.) 3514280A (1985).
155 J.E. Maskasky, "International Congress of Photographic Science", Cologne, September 1986, p. 62, 1986.
156 S. Matsuzaka, Y. Suda and S. Nishiwaki, ibid., p. 65.
157 F.H. Claes, M.J.M. Libeer and W.J. Vanassche, J. Phot. Sci., 21(1973)39.
158 D. Wyrsch, "International Congress of Photographic Science", Rochester, 1978, p. 122, 1978.
159 J.W. Gibbs, "Collected Works", Longmans, New York, 1928.
160 G. Wulff, Z. Krist, 34(1901)449.
161 P. Curie, Bull. Soc. Fr. Mineral., 8(1885)4.
162 T. Sugimoto, J. Colloid Interface Sci., 91(1983)51.
163 T. Sugimoto, Phot. Sci. Eng., 287(1984)137.
164 F. Claes and R. Berendsen, Phot. Korr., 101(1965)37.
165 R.W. Strong and J.S. Wey, Phot. Sci. Eng., 23(1979)344.
166 G.A. Gamlen and D.O. Jordan, J. Chem. Soc., (1953)1435.
167 R.E. Connick and C.P. Coppel, J. Am. Chem. Soc., 81(1959)6389.
168 G. Wada and Y. Kobayashi, Bull. Chem. Soc. Japan, 48(1975)2451.